TECHNICAL REPORT NO. 2

CONSTRUCTION AND OPERATION OF APPARATUS FOR STUDY OF HEAT TRANSFER WITH SURFACE BOILING

BY

WARREN M. ROHSENOW
EDWARD H. SOMMA
PAUL V. OSBORN

FOR

THE OFFICE OF NAVAL RESEARCH
CONTRACT N5ori-07827
NR-035-267
D.I.C. PROJECT NUMBER 6627

JULY 1, 1950

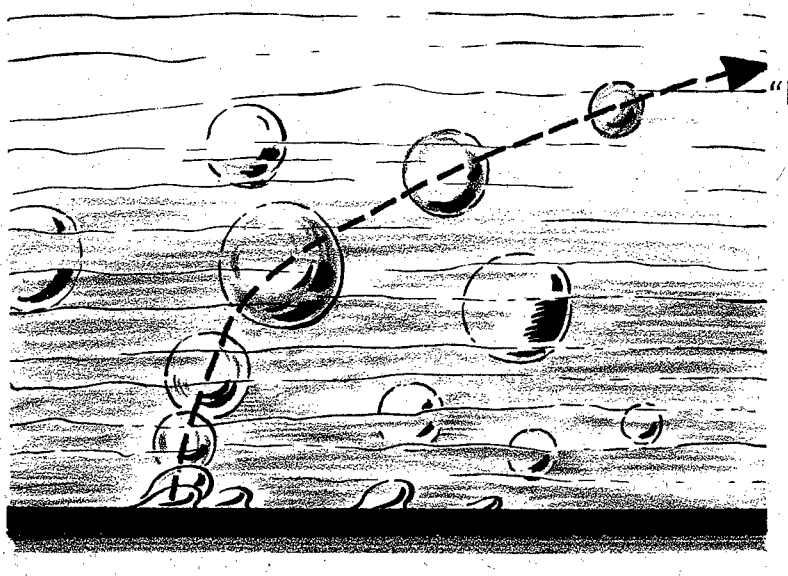

MASSACHUSETTS INSTITUTE OF TECHNOLOGY
DIVISION OF INDUSTRIAL COOPERATION
CAMBRIDGE, MASSACHUSETTS

DISCLAIMER NOTICE

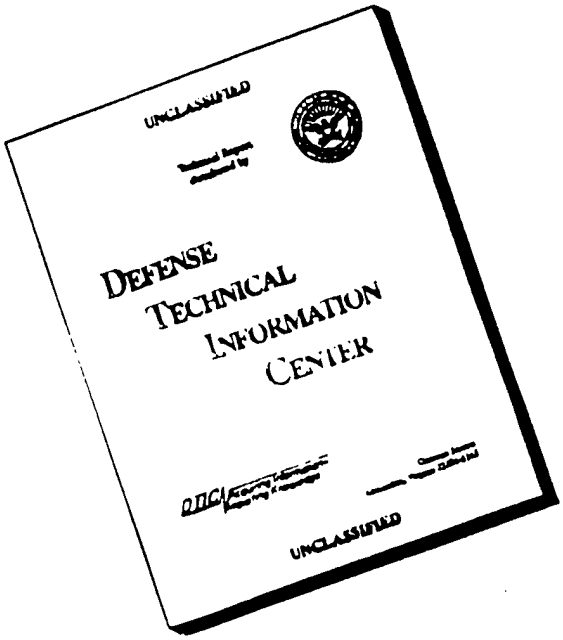

THIS DOCUMENT IS BEST QUALITY AVAILABLE. THE COPY FURNISHED TO DTIC CONTAINED A SIGNIFICANT NUMBER OF PAGES WHICH DO NOT REPRODUCE LEGIBLY.

TECHNICAL REPORT NO. 2

CONSTRUCTION AND OPERATION OF APPARATUS FOR STUDY OF HEAT TRANSFER WITH SURFACE BOILING

by

Warren M. Rohsenow*

Edward H. Somma**

Paul V. Osborn***

For the Office of Naval Research

N 5 ORI - 07827

NR - 035 - 267

DIC PROJECT No.6627

July 1, 1950

DIVISION OF INDUSTRIAL COOPERATION

MASSACHUSETTS INSTITUTE OF TECHNOLOGY

Cambridge, Massachusetts

* Asst. Prof. Mech. Eng. M.I.T., Cambridge, Mass.

** Research Assistant, M.I.T., Cambridge, Mass.

*** Research Assistant, M.I.T., Cambridge, Mass.

PREFACE

The topic of surface boiling of water has become of great importance in recent years because of the increase in applications requiring high rates of heat transfer per unit area. Data is particularly needed in equipment requiring water cooling from temperatures greatly exceeding the boiling point of water at atmospheric pressure.

In order to prevent film binding at the high temperature surface in contact with the cooling water, the pressure of the cooling water can be raised until its saturation temperature is above the wall temperature. However, investigations at low pressures have shown that if the surface temperature is high enough above the saturation temperature, the phenomenon of surface boiling will occur. This has been found to give a marked increase in the heat transfer coefficient over that predicted by well-established forced convection equations, increasing as the surface temperature is increased to a point where film binding and subsequent burnout occurs.

The apparatus described herein was designed to study the effects of surface boiling on heat transfer to water flowing in a tube under the following conditions:

1. Water pressures - up to 2000 psia
2. Water velocities - up to 40 feet/sec
3. Water bulk temperatures - up to 550° F.

SUMMARY

A detailed description of the test apparatus designed and constructed to study the effects of surface boiling on heat transfer at high pressures and high heat flux densities is presented. A discussion is given of operating techniques, data measurements, and calculating procedure with derivations of formulas, calibration of instruments, and other experimental determinations. A series of photographs which record the dismantling of the Hayward-Tyler centrifugal pump for cleaning are presented. They indicate very clearly the source of the contamination which has led to a continual deposition of scale on the inside of the test section, apparently due to an electro-plating of ferric ions. Cleaning of this scale has proven to be exceedingly time consuming and an ion-exchanger to trap the objectionable ions is to be added to the circuit.

DESCRIPTION OF APPARATUS

The procedure for investigating heat transfer with surface boiling consisted of determining the heat flux density q/A for a particular temperature difference driving force at particular values of velocity, pressure, and subcooling, for degassed, distilled water flowing upward in a pure nickel tube. Pressure drops across the test section were also measured.

The test apparatus is a closed system consisting of a vertical test section of pure nickel, a Hayward-Tyler centrifugal pump, a calibrated orifice, a heat exchanger, and a pressure vessel. A layout is given in Fig. 1. Power is supplied from two 36 KW DC Generators driven by 440 volt, 3 phase, AC synchronous motors. The generator outputs are connected in series and provide a range of 0-24 volts and 0-3000 amperes. Thermocouples are located at the inlet and outlet and along the outer wall of the test section, readings being taken by means of a Rubicon potentiometer, Model 2703 and a Rubicon spotlight galvanometer Model 3401-H. A bourdon type Heise pressure gage 0-2000 psi is located at the inlet to the test section. A Barton differential pressure gage 0-150 inches of water is connected across inlet and outlet of the test section to record the pressure drop.

A photograph of the control panel and motor generators is presented in Fig. 2 and the assembled test section is shown in Fig. 3.

Test Section

The test section consists of a pure nickel tube (International Nickel Co. "L" Nickel) of .1805 in. inside diameter, .2101 in. outside diameter, and a length of 9 inches. (Cf Fig. 4). Threaded bushings of "L" nickel are gold soldered to each end of the test section, and make contact with bronze end mounts, which support the test section assembly and carry current from the bussbars.

"L" nickel was chosen because of favorable strength, thermal, resistive, and non-corrosive characteristics. The dimensions were based on the desired heat flux density of approximately 4,000,000 Btu/hr ft^2, while keeping the sum of the pressure and thermal stresses below the yield point(2). The nickel tubing was especially drawn and the total variation in wall thickness was measured to be .0003 in. Appendix C-4 gives the method used to determine the wall thickness to be used in inner wall temperature calculations.

Power Supply

The power supply consists of two 36 KW Chandeysson, 12 volt, 3000 ampere direct current, externally excited generators driven by 440 volt, 3 phase, AC 600 R.P.M. synchronous motors. In order to obtain the maximum heat flux density of 4,330,000 Btu/hr. ft^2 calculated by Barton(2), a maximum current of

2,000 amperes at 21.6 volts is necessary. In addition the generators must be capable of delivering any amount of power from zero to maximum as required.

The method devised to give this wide range of power and thus a wide range of heat flux densities was to connect the generator outputs in series. One generator output is set continuously at 12 volts and the second generator output is added or subtracted to this initial 12 volts. This is accomplished as in Fig. 5 by one control which mechanically couples two potentiometers, wired so that movable contacts approach opposite polarities. Thus at mid setting, generator #1 field voltage is zero giving a total voltage output of 12 volts, obtained from generator #2. At one extreme position of the potentiometers, full generator #1 exciter voltage is impressed across generator #1 field, adding 12 volts to generator #2, and giving a total output of 24 volts. At the other extreme position, full generator #1 exciter voltage of opposite polarity is impressed across generator #1 field, subtracting 12 volts from generator #2, and giving a total output of zero volts. Thus the entire range of voltage from 0-24 volts is covered easily with one control.

The two generators are started together, with the potentiometer circuit open and replaced by two starting resistors set to give a zero voltage output. (Cf. Figs. 5 and 6). This is done to insure that no voltage will be impressed upon the test section if the potentiometer control is not zeroed before starting. This could cause a burnout of the test section if, for example, cooling water flow were insufficient. A relay is then energized which pulls out the starting resistors and substitutes the potentiometers.

A master stop button is provided for emergency use in shutting down all electrical equipment with the exception of the silicone heat exchanger pump.

Circulating Pump

The test water circulating pump is a four stage all "stainless" centrifugal pump, manufactured by Hayward-Tyler and Company, Ltd. of England, represented in this country by the DeLaval Steam Turbine Co. of Trenton, N. J. A drawing of the pump and characteristic curves are shown in Figs. 7 and 8.

This pump is of the submersible type, that is, the entire impeller and motor assembly is enclosed in a single, large, stainless steel casing. This has the advantage that there are no rotating shafts of any kind requiring high pressure, high temperature seals. The only two seals in the pump are metal to metal contact between the outer motor casing and the center assembly and between the impeller casing and the center assembly. A series of large studs sledged tight, makes the possibility of leaks very remote.

The main disadvantage of this pump is the fact that the motor is constructed of iron-silicon and the motor cooling water which circulates between it and the stainless casing has corroded the motor considerably. The motor cooling water is circulated through its own heat exchanger but between the motor cooling water and the pump test water below, there are four holes of about 3/8 in. diameter. They are intended to transmit pressure with little exchange of water. However, upon shutting down the pump it was found that some contamination did seep down, necessitating complete draining and refilling before each run.

The pump had been filled with an oil before shipment which could not entirely be removed by flushing. This necessitated dismantling the entire pump. The dismantling was also desired since a sister pump located at the University of California of Los Angeles had experienced galling between wearing rings and impellers, and investigation found particles of sand in the stainless steel castings, traces of which had been found in the test water previously. Mr. K. N. Woodward of the De Laval Company supervised this work, a complete report of which is found in Appendix D.

After dismantling, cleaning, and reassembling, the pump was run for approximately forty hours through the closed loop without the test section. There was no seizing or stalling and the pump delivered its rated load. It was noted that distilled water of conductivity 1 part per million as NaCl became contaminated after as little as four hours in the pump. The lowest conductivity ever recorded after a daily run was 4 p.p.m. The cause of this has been determined to be ferric ions.

It was decided to use the pump as it was, with freshly distilled, degassed water before each run and to check with well established forced convection equations before proceeding to the surface boiling region. No data could be found pertaining to the effects of electrical conductivity of the test water on heat transfer coefficients, and it was hoped that the effect would be slight.

Heat Exchanger

The function of the heat exchanger in the test loop is to remove the heat transferred to the test water in the test section so that the same water can be recirculated continuously. Since the maximum heat input contemplated is approximately 50 KW(2), the heat exchanger must have a capacity of 50 KW or 170,600 Btu/hr.

The final design arrived at(2) consists of two counter-flow heat exchangers, one between the test water and silicone fluid DC-701 (Dow Corning Corp.), the second between the silicone fluid and city water. The boiling point of DC-701 silicone is 572°F at atmospheric pressure and since the maximum inlet temperature of the test water into the heat exchanger is about 586°F, there is no danger of film binding at the coolant contact surface, which would be the case if city water were used instead of silicone fluid.

The first heat exchanger consists of a tube in tube unit, with the test water flowing through a 3/8 inch 18 B.W.G. type 304 stainless tube and the silicone flowing through a 3/4 inch standard wrought iron pipe (.824 in. I.D.). The second heat exchanger consists of a bundle of three 1/2 inch, 20 B.W.G. copper tubes through which the silicone flows and an annulus of 1-1/2 inch 16 B.W.G. copper tubing through which the city water flows. The silicone is circulated by a Worthington gear pump, type 3 GAM. A valved bypass is provided around the test water to silicone heat exchanger, and can be opened at low silicone flows so as not to overload the pump motor. A layout of the two heat exchangers is given in Fig. 9.

Four Vapor Tension thermometers (U. S. States Gauge Type 907S) are located at the heat exchanger inlets and outlets. These are provided as a precaution to insure that the city water leaving the city water-silicone heat exchanger does not reach the boiling temperature, and to insure that the silicone leaving the test water-silicone heat exchanger does not exceed the boiling temperature of water, for fear of vapor binding at the city water surface.

As a further precautionary measure, a pressure switch connected to warning lights at the main control panel is located at each heat exchanger outlet. These provide warning in the event of a city water failure, a failure of the Worthington pump, or the loss of the silicone fluid. At the same time, it provides a reminder to turn on the silicone pump and to open the city water valve before putting any power into the test section.

Pressure Vessel

The purpose of the pressure vessel is to provide a range of system pressures up to 2000 psia and to provide makeup water in the event of small leaks. A layout of the pressure vessel is given in Fig. 10. It consists of a five foot length of type 304 stainless steel seamless tubing, outside diameter 6.180 inches, inside diameter 4.980 inches, with 2 inch plates welded at the ends. The odd sized dimensions were not chosen particularly, but are a result of the inability to locate any other size with the heavy wall thickness needed to withstand the required pressure.

Pressure is built up by boiling water in the vessel by means of 8 110 volt AC, 1.5 KW strip heaters (Chromalox #T 15424) bent into a U shape, surrounding the vessel. In order to obtain a good heat transfer surface, molten aluminum was cast around the heaters into a sheet metal mold. The entire range of 0-12 KW can be utilised by means of individual toggle switches and a variac across one heater. Once the desired pressure has been reached, the proper combination of heaters plus variac setting will keep the pressure vessel at equilibrium.

Enough insulation has been used so that the heat loss to the atmosphere is fairly small, about 2 KW at 1500 psia, yet great enough to give flexibility in decreasing the pressure.

Instrumentation

Flow Measurements

Test water flow rates are determined by measuring the differential pressure across a calibrated orifice (Cf. Appendix C-1) by means of a Barton Differential Pressure Gage.

This gage is constructed of all stainless steel parts, and although rated at 1500 psi, has been tested to 2200 psi. A sectional view of the instrument is shown in Fig. 11. The range of this gage is 0-100 inches of water and was checked at atmospheric pressure by a water manometer. (Cf.Fig.12)

The accuracy of the instrument is within ± 1% of full scale reading.

Pressure Vessel Liquid Level Measurements

It is very important that enough water be put into the pressure vessel initially to insure a sufficient contact surface with the heated walls for quick pressure build-ups. If too much water is put in initially, there arises the danger of completely filling the vessel due to thermal expansion of the water and rupturing the vessel.

A liquid level indicator that would withstand pressures up to 2000 psi and give a remote panel reading was devised, using another Barton Differential Pressure Cage with a reversed reading scale 50-0 inches of water. A schematic diagram of the indicator is given in Fig. 13.

During a filling prior to a run, the pressure vessel is filled with valve 1 open, thus insuring that the bypass loop is also filled. The valve is then closed giving a constant head of water at gage port 2. The head at port 1 is variable, depending on the height of water in the vessel. The gage reading is then a direct function of the height of water in the pressure vessel, regardless of the vapor pressure, which cancels out by being additive to each side of the gage. It will be noted that at the minimum indicated level reading, the differential pressure across the gage is a maximum, and at the maximum indicated level reading, the differential pressure is a minimum.

The one serious consideration that must be given this type liquid level indicator is that of varying densities of water at various saturation temperatures. There is the danger that the vessel might be full at some higher temperature than calibrated and yet read several inches lower than full, due to a lower water density. This was overcome by calculating the gage readings for a pressure vessel full of water at various saturation pressures up to 2000 psia. These maximum safe gage readings were never exceeded for any particular operating pressure.

Power Measurements

The purpose of the power measurements is to accurately determine the heat flux density q/A, and to determine the test section current, one of the variables used in calculating the test section inner wall temperatures.

Current is measured by means of the voltage developed across a standard resistor shunt. Four 50 millivolt, 3000 ampere General Electric shunts were supplied with the motor-generators and one of these was sent to the National Bureau of Standards for calibration. (Cf. Fig. 14). The shunt is constructed of manganin, which has a flat resistance versus temperature curve, but still rises slightly in resistance at higher temperatures. The shunt was mounted with the vanes vertically to enhance natural circulation and all copper busbar connections were utilized to increase conduction. The result was that the shunt remained at approximately 100°F even when 3000 amperes passed through it. The voltage across the shunt was measured with a Rubicon

Potentiometer. The value of the current in terms of the potentiometer reading is shown below:

$$I = \frac{E}{R} = \frac{.001}{.00001662} = 60.17 \text{ amps/millivolt}$$

Voltage measurements across the test section were also made by means of the potentiometer, with a voltage divider network utilized to scale down the voltage to a value that could be read on a 50 millivolt potentiometer. The circuit is illustrated in Fig. 15. The resistors used in the circuit were purchased from the General Radio Company in Cambridge, Mass. and calibrated by the Electrical Instrument Laboratory at M.I.T. The results of the calibration are:

Resistor	Resistance
500B 10 ohms	9.994 ohms (R_1)
500M 5000 ohms	5003.5 ohms (R_2)

The potential taps to the test section were made of nickel and held in place by a stainless steel spring mechanism. The taps and leads were made of nickel in order to reduce thermal EMF's. The resistance of the leads was approximately 1.0 ohms, shown schematically as R_3 in Fig. 15.

The voltage across R_1 is related to the voltage across the test section in the following manner:

$$E_{ts} = E_1 \frac{R_1 + R_2 + R_3}{R_1} = 501.8\, E_1$$

$$E_{ts} = .5018 \text{ volts/millivolt}$$

Test Section Outer Wall Temperature Measurements

Measuring the outer wall temperature of the test section presented several problems, and several solutions to the problem were investigated before the method in use on the apparatus was developed. In viewing the overall problem, the following considerations should be kept in mind:

1. A thermocouple in intimate contact with a tube wall of 0.015 in. thickness by being welded or silver soldered would disturb the local current distribution and give erroneous temperature readings. In addition, a thermocouple welded to the test section might result in stress concentrations which

would rupture the tube at high pressures and temperatures.

2. Since the tube is heated with direct current, a thermocouple in electrical contact with the tube would have impressed across it a potential attributable to the voltage gradient at that point. This would necessitate reversing the direction of current to determine the thermal EMF alone.

3. Thermocouples not welded to the test section will be in a region of high temperature gradient from the wall to the surrounding air, and will give temperature readings below that of the wall. Any electrical insulation placed between the wall and the thermocouple will add to the error.

The method in use on the apparatus is illustrated in Fig. 16. Twelve thermocouples are bound to the tube wall with fiberglass cord. A photograph of a bound test section is given in Fig. 17. Placed between each thermocouple and the tube wall is a small sheet of.0015 in. mica to insulate the two electrically. Around the tube, filled with a high temperature insulation Kaolin wool, is an electrically heated copper shield, made in three sections, each controlled by a variac. Three thermocouples are silver soldered to the shield as shown in Fig. 16.

When the shield temperature is adjusted to the same temperature as the test section outer wall, the space between should also be at this temperature. There should then be no temperature gradient across the thermocouples, which would read the correct outer wall temperature. Kreith and Summerfield (3) and McAdams (4) report that with surface boiling, the outer wall of the test section is at a fairly uniform temperature. Thus a uniform setting of the shield temperatures for any one set of conditions should result in accurately read wall temperatures. In the non-boiling region of heat transfer, the test section will have a considerable axial temperature gradient, so that all three variacs can be adjusted to follow fairly closely the tube temperatures. A discussion of tube temperature errors as found in a mock-up of the test section is given in Appendix C-5.

Test Section Pressure Drop Measurements

Pressure drop across the test section is measured by means of a Barton Differential Pressure Gage, 0-150 inches of water, connected at the pressure taps as shown in Fig. 4. The temperature of the water in the vertical test section is considerably higher than the temperature of the ambient water in the gage lead-in tubing, necessitating a correction factor to determine the actual friction pressure drop. The equation for converting gage readings to friction pressure drop is as follows:

$$\Delta P_f = \Delta P_g + \frac{(62.4 - \gamma_b)}{62.4} \times \text{Distance between pressure taps}$$

EXPERIMENTAL PROCEDURE

Degassed, distilled water is used in all runs. Distilled water of conductivity 0.7 ppm is degassed by boiling in a stainless steel container heated by a steam coil. The system is filled, and the water is circulated through the pressure vessel and heated to boiling. This drives any air trapped in the loop into the pressure vessel, which is vented to the atmosphere.

The system pressure is then raised to the desired level by boiling the water in the pressure vessel. The system throttle valve is adjusted to the approximate flow desired, slight changes being necessary as bulk temperatures change. The direct-current generators are now energized, and approximately 500 amperes is passed through the test section without the heat exchangers operating. When the bulk temperature of the water has reached the desired value, the heat exchangers are put into operation.

The power input to the test section is gradually increased while adjusting the heat exchangers, throttle valve, and pressure vessel heaters to maintain the desired values of velocity, pressure, and subcooling. Preliminary data is taken continuously in order to determine when steady state conditions have been attained.

Several sets of data are taken at each equilibrium condition in an effort to detect any possible transients, and to minimize human errors in reading instruments. In order to obtain an entire curve in as few runs as possible, the pressure and velocity are kept constant as the power input is increased. The water bulk temperature is allowed to vary slightly within a range which will keep the desired bulk temperature somewhere within the test section. This can be done because of the method of point-wise calculation which determines the heat flux density q/A, the inside wall temperature t_w, and the bulk temperature t_b at seven points along the tube.

In an effort to follow each run more closely, a number of curves and charts were prepared in advance which convert outside wall temperatures to inside wall temperatures, power to q/A in Btu/hr ft^2, potentiometer readings to temperatures, and differential pressure gage readings to water velocity in feet/sec. From the Colburn equation, curves of q/A versus t_w-t_b had been plotted for the particular operating conditions, and data points are spotted on the curve as they are obtained.

Test Section Outer Wall Temperature Measurements

In order to obtain accurate wall temperature measurements using the method of a heated shield, it is important that the shield and the outer wall of the test section be at the same temperature. This method had been developed on the assumption that an almost uniform outer wall temperature would be found at the condition of surface boiling.

It was found, however, that the wall temperatures increased from inlet to outlet, with a maximum increase of 400°F found in Run 8. That particular test section was found to have the thickest deposit of scale (5), other runs varying from clean to slightly contaminated tubes. To obtain accurate temperature measurements, each section of the heated shield is set equal to the outer wall thermocouple opposite it. From Fig. 28, the error in outer wall reading is seen to be less than 5°F if the shield temperature differs from the tube temperature by as much as 65°F.

A technique of reaching equilibrium quickly between each shield section and its opposite tube temperature was developed. It is accomplished by overshooting the controlling variac in the direction of change, and then backing off quickly when the desired temperature is reached. Each shield section has a small effect on its neighbor but no great difficulty in obtaining the proper temperatures has been experienced.

Test Water Air Content Analysis

The Winkler technique is used to determine the quantity of oxygen dissolved in the test water. The dissolved air is calculated from the ratio of the Henry's law constant for air and oxygen in water.

A wide mouth, glass stoppered, 250 cc bottle is used for the sampling and subsequent chemical analysis. The test water is introduced through a rubber tube into the bottom of the bottle, and the water is allowed to overflow for several minutes to insure that the water which had come in contact with the air will be removed.

The chemical reagents which are used consisted of the following:

1. 480 gm. $MnSO_4$ in one liter water
2. 100 gm. NaOH and 360 gm. KI in one liter water
3. Concentrated H_2SO_4 diluted 1:1 with distilled water
4. 5 gm. Starch in 100 cc water
5. Standard solution $Na_2S_2O_3$ (approximately .01 Normal)

The procedure followed is to add 2 cc of reagents 1, 2 and 3 in that order to the 250 cc water sample. A few cc of starch solution 4 is added which turns the color blue. 100 cc of this blue solution is then titrated with reagent 5, the standard solution of $Na_2S_2O_3$.

The chemical reagents are added through graduated pipettes placed at the bottom of the sample. The 2 cc of each reagent displaced a like amount

at the bottle mouth, and it was hoped that this method would remove most of the error that would be obtained by oxygen dissolving at the water surface. No further precautions are observed after the H_2SO_4 is added as further oxygen dissolved in the sample has no effect on the amount of titration.

The equation below relates the amount of oxygen in parts per million by weight to the normality and number of cubic centimeters of $Na_2S_2O_3$ titrated.

$$O_2 = 80\ (N)\ (cc)$$ and:

$$Air = 2.9\ O_2$$

CALCULATION PROCEDURE

All sample calculations are based on Run 7-13 with the mid-point of the test section (station 4) being used for all calculations.

1. Inside wall temperature

The plot shown in Fig. 18 is used to determine $t_o - t_w$ from the current and t_o.

$t_o = 474°F$, $I = 1245$ amps, $t_o - t_w = 22°F$

$t_w = 452°F$

2. Mean Resistivity

Resistivity is plotted in Fig. 23 as a function of the temperature. The mean resistivity at station 4 is assumed to be that evaluated at the mean wall temperature, $(t_o + t_w)/2$.

$$(t_o + t_w)/2 = (474 + 452)/2 = 463°F$$

$$\rho_m = 6.75 (10^{-7}) \text{ ohm-feet}$$

3. Heat Flux Density

$$q/A = 1.148 (10^6) I^2 \rho_m$$

$$q/A = 1.148 (10^6)(1245)^2 (6.75)(10^{-7})$$

$$q/A = 1,201,000 \text{ Btu/hr ft}^2$$

4. Average Heat Flux Density

$$(q/A)_{avg} = \frac{3.413 E I}{\pi L D_i}$$

$$(q/A)_{avg} = \frac{3.413(10.54)(1245)}{3.14 \left(\frac{9.13}{12}\right)\left(\frac{.1605}{12}\right)}$$

$$(q/A)_{avg} = 1,252,000 \text{ Btu/hr ft}^2$$

5. Bulk Temperature (Cf App. B-3)

$$t_{b4} = t_{in} + (t_{b1} - t_{in}) + (t_{b2} - t_{b1}) + (t_{b3} - t_{b2}) + (t_{b4} - t_{b3})$$

$$t_{b4} = t_{in} + \frac{\pi D_i}{\omega c_p} \sum (q/A)_{III-1} X_{III-1} + (q/A)_{1-2} X_{1-2} + (q/A)_{2-3} X_{2-3} + (q/A)_{3-4} X_{3-4}$$

$$t_{b4} = 208 + \frac{(3.14)(.015)}{(630)(1.02)} \sum (9 \times 10^5)\left(\frac{.99}{12}\right) + (9.7 \times 10^5)\left(\frac{1.40}{12}\right) + (10.6 \times 10^5)\left(\frac{1.40}{12}\right) + (11.6 \times 10^5)\left(\frac{1.40}{12}\right)$$

$$t_{b4} = 237\,^\circ F$$

6. Temperature Driving Force

$$t_w - t_b = 452 - 237$$

$$t_w - t_b = 215\,^\circ F$$

7. Surface Heat Transfer Coefficient

$$h = \frac{q/A}{t_w - t_b} = \frac{1,201,000}{215}$$

$$h = 5,600 \text{ Btu/hr ft}^2\,^\circ F$$

8. Subcooling

$$t_{sub} = t_{sat} - t_{b4} = 385 - 237$$

$$t_{sub} = 148\,^\circ F$$

9. Nusselt Number

$$Nu = \frac{hD_i}{K} = \frac{(5600)(.015)}{.396}$$

$$Nu = 212$$

10. Prandtl Number

$$Pr = \frac{c_p \mu}{K} = \frac{(1.02)(.59)}{.396}$$

$$Pr = 1.51$$

11. Reynolds Number

$$Re = \frac{wD_i}{\mu A} = \frac{(630)(.015)}{(.59)(.000177)}$$

$$Re = 89,500$$

12. Nusselt Number from the Colburn Equation

$$Nu = .023\, Re^{.8} P_r^{1/3}$$

$$Nu = .023\,(89,500)^{.8}(1.51)^{1/3}$$

$$Nu = 254$$

13. Pressure Drop Across Heated Portion of Test Section

To obtain the friction pressure drop across the heated portion of the test section, two corrections must be made to the Barton differential pressure gage reading. The pressure drop across the unheated portions of the test section must be subtracted from the total reading, and correction must be made for the difference in densities between the liquid within the test section and the liquid in the lines connecting the gage across the test section.

a. No Surface Boiling

$$\Delta P_{ts} = \Delta P_g + \frac{(62.4-\gamma_b)L_t}{62.4} - \frac{(L_t-L_h)}{L_t}\left[\Delta P_g + \frac{(62.4-\gamma_b)L_t}{62.4}\right]$$

$$\Delta P_{ts} = 58.5 + \frac{62.4-59}{62.4}(13.12) - \frac{(13.12-9.38)}{13.12}(59.2)$$

$$\Delta P_{ts} = 42.5 \text{ in. } H_2O$$

b. Surface Boiling

The pressure drop under conditions of surface boiling cannot be accurately calculated since the unknown quantity of vapor within the test section makes the average density uncertain. If the density is assumed to change a negligible amount as far as pressure drop is concerned, the following equation is a good approximation. Calculations are based upon Run 7-17.

$$\Delta P_{ts} = \Delta P_g + \frac{(62.4-\gamma_b)}{62.4}L_t - \frac{(L_t-L_h)}{L_t}\left[\Delta P_{nb} + \frac{(62.4-\gamma_b)}{62.4}L_t\right]$$

$$\Delta P_{ts} = 96 + \frac{(62.4-57.2)}{62.4}(13.12) - \frac{(13.12-9.38)}{13.12}\left[58.5 + \frac{(62.4-57.2)}{62.4}13.12\right]$$

$$\Delta P_{ts} = 80.5 \text{ in. } H_2O$$

APPENDIX A

NOMENCLATURE

A	Area, sq feet
A	Heat transfer area, sq feet
c_p	Specific heat, Btu/lb ^{o}F
D	Diameter, feet
D_i	Inner diameter of test section, feet
$\frac{de}{dx}$	Voltage gradient, volts/ft
E	Test section voltage, volts
G	Mass velocity, lb/hr ft^2
h	Surface coefficient of heat transfer, Btu/hr ft^2 ^{o}F
I	Test Section Current, amperes
k	Thermal Conductivity, Btu/hr ft ^{o}F
L	Test section length between potential taps, 9.13 inches
L_h	Test section heated length, 9.38 inches
L_t	Test section total length, 13.12 inches
Nu	Nusselt number
P	Pressure, psia
ΔP_g	Pressure drop reading across test section, in. H_2O
ΔP_{nb}	Pressure drop reading across test section with no boiling, in. H_2O
ΔP_{ts}	Pressure drop across heated portion of test section
Pr	Prandtl number
q/A	Heat flux density, Btu/hr ft^2
r_o	Outer radius of test section, feet
r_i	Inner radius of test section, feet

R	Resistance, ohms
Re	Reynolds number
t_b	Test water bulk temperature, ^oF
t_{in}	Test water inlet bulk temperature, ^oF
t_{out}	Test water outlet bulk temperature, ^oF
t_o	Test section outer wall temperature, ^oF
t_w	Test section inner wall temperature, ^oF
t_{sat}	Saturation temperature, ^oF
t_{sh}	Heated shield temperature, ^oF
ΔT	Temperature driving force, $t_w - t_b$, ^oF
V	Flow velocity, feet/sec
w	Flow rate, lb/hr
X	Distance between thermocouple stations, 1.4 inches
α_ρ	Temperature coefficient of electrical resistivity, $^oF^{-1}$
α_k	Temperature coefficient of thermal conductivity, $^oF^{-1}$
α_T	Temperature coefficient of thermal expansion, $^oF^{-1}$
γ	Density, lb/cu ft
γ_b	Density at bulk temperature, lb/cu ft
ρ	Electrical resistivity, ohm feet
ρ_m	Electrical resistivity at temperature $\frac{t_o + t_w}{2}$
μ	Viscosity, lb/hr ft

APPENDIX B

DERIVATIONS OF FORMULA

1. Inner Wall Temperature

The equation used for calculating the inner wall temperature was derived by Kreith and Summerfield [3] and is given below:

$$t_w = t_o - \frac{m(r_o-r_i)^2}{(1+\alpha_\rho t_o)(1+\alpha_K t_o)} - \frac{m(r_o-r_i)^3}{3r_o(1+\alpha_\rho t_o)(1+\alpha_K t_o)}$$

$$- \left[\frac{m^2(3\alpha_K + 4\alpha_\rho\alpha_K t_o + \alpha_\rho)}{6(1+\alpha_\rho t_o)^3(1+\alpha_K t_o)^3} + \frac{m}{4r_o^2(1+\alpha_\rho t_o)(1+\alpha_K t_o)}\right](r_o-r_i)^4$$

where

$$m = \frac{3.413\left(\frac{de}{dx}\right)^2}{2\rho_o K_o}$$

Since the electrical resistivity of L nickel varies so widely with temperature, the voltage gradient along the tube de/dx will vary considerably. To avoid the installation of a series of potential taps along the test section to determine the voltage gradient at each thermocouple, the equation was put in terms of current, the average value of which is constant at all cross-sections. The conversion is as follows:

$$\frac{de}{dx} = \frac{I\rho_m}{A} = \frac{I\rho_m}{\pi(r_o^2 - r_i^2)}$$

$$m = \frac{3.413\,\rho_m^2 I^2}{2\rho_o K_o \pi^2 (r_o^2 - r_i^2)^2}$$

The equation has been plotted in Fig. 18 as $t_o - t_w$ versus I at various levels of t_o.

2. Heat Flux Density q/A

The power dissipated in any portion of the test section is dependent upon the resistance, which, being a function of temperature, varies from point to point along the tube. The heat flux density then varies along the test section length and must be calculated to obtain accurate results.

The equation below is derived for the calculation of q/A as a function of the energy and the wall resistivity of a small element of tubing dx.

$$q/A = \frac{3413\, I^2 R}{A_s} = \frac{3.413\, I^2 \rho_m\, dx}{\pi D_i\, dx\, \pi (r_o^2 - r_i^2)}$$

$$q/A = 1.148 (10^6) I^2 \rho_m$$

3. Test Water Bulk Temperature

Since the heat flux density varies considerably along the test section length, it is not sufficient to assume a linear increase in the test water temperature from inlet to outlet. As an example, an error of 3% in the temperature driving force is introduced in Run 7-13 by making this assumption.

A more exact method of finding t_b is based upon the integration of q/A over the area from the inlet to the station in question. For the derivation of the equation two assumptions are necessary, that there is no significant heat flow axially along the tube, and that during surface boiling the vapor generated within the tube does not appreciably change the average specific heat of the water.

The energy balance between the electrical energy dissipated in a small element of tubing dx and the corresponding temperature rise of the water is expressed in the equation below:

$$c_p w\, dt_b = q/A\, dA = q/A\, \pi D_i\, dx$$

Rearranging the terms and integrating:

$$\int dt_b = \frac{\pi D_i}{c_p w} \int q/A\, dx$$

For purposes of graphical integration, q/A is plotted at the thermocouple stations along the test section as illustrated in Fig. 19. Between any two stations, n and n-1, q/A is assumed to vary linearly. The mean q/A is:

$$(q/A)_{n-(n-1)} = \frac{(q/A)_n + (q/A)_{n-1}}{2}$$

and the equation for the temperature rise between any two stations is:

$$t_{bn} - t_{b(n-1)} = \frac{\pi D_i}{c_p w} (q/A)_{n-(n-1)} X_{n-(n-1)}$$

Data taken with the apparatus affords several checks of this equation. The q/A_{avg}, calculated from the power measurement should be equal to the average height of the q/A versus length plot, and the sum of the water temperature rises between stations should be equal to $t_{out}-t_{in}$.

APPENDIX C

CALIBRATIONS AND EXPERIMENTAL DETERMINATIONS

1. Orifice Calibrations

The range of flows to be covered was estimated to be from 300 to 1300 pounds of water per hour, which corresponds to velocities through the test section of 10 to 40 feet per second. Two orifice plates and a Barton Differential Pressure Gage, 0-100 inches of water, were obtained to cover this range. To insure the accuracy of the flow measurements, the orifice plates were calibrated.

The system used for the calibration consisted of a centrifugal pump as a source of pressure, a valve regulating the flow, and the Barton gage measuring the pressure drop across the orifice, and a weighing tank.

The formula relating the flow and the pressure drop across the orifice is:

$$w = \gamma A C \sqrt{\frac{2g\Delta P}{\gamma}} = C_1 \sqrt{\gamma \Delta P}$$

C_1 for any given orifice is a function of the Reynolds number at low Reynolds numbers, but remains constant at higher values. The flows to be measured are all at the higher Reynolds numbers, making C_1 a constant throughout the entire range.

Data obtained in these calibrations is presented on the following page. Curves of flow in pounds per hour versus Barton gage reading have been plotted in Fig. 20. From these curves, velocity through the test section in feet per second versus Barton Gage reading have been plotted in Fig. 21.

Inches of Water	Lbs. per Hour	Reynolds Number	C_1
10	458	12,800	18.35
15	555	15,500	18.15
20	639	17,850	18.10
30	784	21,900	18.18
40	914	25,600	18.30
50	1023	28,600	18.35
60	1115	31,200	18.28
70	1200	33,500	18.20
		Average	18.24

Low Range Orifice

Inches of Water	Lbs. per Hour	Reynolds Number	C_1
10.1	152.5	6,940	6.08
20.0	219	10,000	6.20
30.8	268	12,200	6.13
40.2	306	13,900	6.14
50.3	343	15,600	6.12
60.4	375	17,000	6.11
81.0	430	19,500	6.08
96.0	462	21,000	5.99
99.5	474	21,500	6.03
		Average	6.10

2. Nickel Resistivity Measurement

An accurate knowledge of the resistivity and thermal conductivity of L nickel as a function of temperature is necessary for the calculation of the inner wall temperature of the test section. Data obtained from the International Nickel Company in a private communication was deemed satisfactory for the thermal conductivity, (Cf. Fig. 24) but resistivity was stated to vary slightly from heat-to-heat. Therefore measurements of the resistivity of the nickel tubing drawn for us were made at various temperatures to determine the values for the particular tubing.

A schematic diagram of the apparatus used is shown in Fig. 22. The nickel tubing was maintained at various temperature levels in an electrically heated furnace. Three thermocouples were placed longitudinally along the tube for temperature determination. The tube, a standard resistor of .01 ohms, and a variable rheostat were connected in series across a 2 volt storage battery. Since the current in the loop is constant, the ratio of the resistance of a length of the tube to that of the standard resistor are proportional to the voltage drop across each.

A Rubicon semi-precision potentiometer was used to measure these voltage drops at various temperatures. The potential taps were placed on the tubes sufficiently far from the calibrating current terminals to insure symmetrical current flow at any cross section of the tube between potential taps. The lead-in wires were made of nickel to reduce thermal EMF's.

The rheostat was placed in the circuit to drop the excess battery voltage and to allow for variation of the calibrating current and hence the magnitude of the voltages being measured. This served as a check, since the ratio of the two voltage drops should be a constant at any particular temperature, regardless of the level of current.

The thermocouples along the tube indicated a maximum variation in temperature of 17°F end to end at a temperature level of 800°F. The average value of the three temperatures was used. Small thermal EMF's were registered across the length of the tube when the calibrating current was reduced to zero. These were subtracted from the potentiometer readings to obtain the voltage drop due to current alone. The ratio of the two voltage drops remained constant at a particular temperature to within .5% at various magnitudes of current.

Data

Temperature(°F)	Tube Resistance (Ohms 10^{-2})
75	2.955
216	4.105
324	5.158
365	5.598
465	6.750
506	7.291
615	8.963
668	9.950
701	10.459
757	10.925
807	11.265

Calculations

The resistivity of a length of the tube is defined by the following relation:

$$\rho = \frac{RA}{L}$$

Since the area and length are a function of temperature, the equation is expanded to:

$$\rho = \frac{RA_0(1+\alpha_T \Delta t)^2}{L_0(1+\alpha_T \Delta t)} = \frac{RA_0}{L_0}(1+\alpha_T \Delta t)$$

The cross-sectional area of the tube was calculated from measurements of length and weight and from known density. (Cf App. C-4)

Results. (Plotted in Fig. 23)

Temperature ($^\circ$F)	Resistivity (ohm-feet x 10^{-7})
75	2.961
216	4.117
324	5.179
365	5.620
465	6.784
506	7.327
615	9.017
668	10.009
701	10.532
757	11.001
807	11.344

3. Thermocouple Calibration

Thermocouples of Chromel P and Constantan were used for temperature measurements. These metals were chosen for their high thermal EMF per degree of temperature difference, and for stability at temperatures to 800°F.

The thermocouples were calibrated at the Heat Measurements Laboratory at the Massachusetts Institute of Technology. Apparatus is set up there for calibrating thermocouples at the temperatures of condensing steam, condensing naphtha, condensing mercury, and condensing sulfur. In addition, there is a large copper block that is maintained electrically at approximately 1200°F in which thermocouples can be calibrated against a standard Copper-Constantan thermocouple. It was felt that this number of points would be adequate to give temperatures of $\pm$.5% from 32-800°F when the thermal EMF is measured by a precise potentiometer and galvanometer.

Thermal EMF is plotted against temperature in Fig. 25. This plot is insufficient for accuracies of the order of .5% since many good looking curves can be plotted through these points which will exceed this error. It is necessary to calculate a mathematical curve which passes through these points, or to plot a deviation curve from the National Bureau of Standards curve for the same type thermocouple.

Fig. 26 is a plot of the deviation of the calibrated thermocouple from the Bureau of Standards data given in Tables 19, 20, and 21 of "Tables of Thermocouple Characteristics", a General Electric Publication (GET-1415). These tables were derived from Bureau of Standards data on Chromel-Platinum and Constantan-Platinum thermocouples.

Calibration Data

Apparatus	Temp. °F	Thermal EMF(mv)
Copper Comparator	117.36	2.78
Steam Condenser	211.8	6.08
Naphtha Condenser	423.8	14.18
Mercury Condenser	673.3	24.48
Sulfur Condenser	831.7	31.19

4. Wall Thickness Determination

In order to accurately calculate the inner wall temperature at any point along the test section, the wall thickness and the outer wall temperature at that point must be accurately known. This would necessitate a delicate measuring device which could probe into a .180 in. diameter to a depth of at least half the test section length, and map the wall thickness at points where thermocouples were to be placed.

It was felt that the accuracy obtained did not warrant such painstaking instrumentation since thermocouples were to be placed at intervals along and around the tube, and knowing the precise inner wall temperature at a few selected points only would not give any more accurate results. It was felt that the average wall thickness of the entire test section would give as meaningful results.

From known density, and measured weight, length, and outside tube diameter of .2101 in., the average inner diameter was calculated to be .1805 inches. The average wall thickness was then calculated to be .0148 inches.

5. Mock-Up For Test of Temperature Measuring Apparatus

A mock-up of the test section was built to determine the operating characteristics of the heated shield method of surface temperature measurements.

The characteristics of special interest were:

1. Tolerances of the shield temperature which would permit $1^{\circ}F$ accuracy using thermocouples bound to the outer tube wall.

2. The axial temperature distribution of the shield. Cooling effects of the end supports might place too great a temperature gradient in the shield axially which would introduce errors in measuring the outer walls.

3. Time increments necessary to achieve steady state with the shield at the same temperature as the test section. If the time necessary to come to equilibrium is too great, data taking, the bulk of which is the test section outer wall temperature, will be slowed down considerably.

In order for a mock-up to be of any value, it should approach as closely as possible the actual operating characteristics of the ultimate installation. Since the actual apparatus had not been fully constructed, it was necessary to rely partly on the reports of other investigators (3),(4) in determining what the actual operating characteristics might be in the surface boiling region.

The prime prerequisite was thought to be a tube of constant axial temperature to resemble surface boiling conditions. Another important prerequisite was a constant temperature tube regardless of surrounding atmospheric temperatures. This was determined from the fact that in the ultimate installation, the amount of heat loss from the outer wall is so small compared to the heat flowing from the inside wall to the water, that its magnitude will not affect the outer wall temperature at all. Therefore, the actual outer wall temperature of the tube will not be affected by changes in the shield temperature, only the thermocouple readings will be affected.

To achieve these conditions it was decided to pass condensing vapor through a nickel tube having the same dimensions as the test section. The surface heat transfer coefficient between a condensing vapor and the inside surface of the tube is sufficiently high that any cooling or heating effect by the shield surrounding the tube will not change the tube temperature from that of the condensing vapor. As long as the condensing vapor is in the two phase region along the entire length of the tube, the temperature along the entire length will be uniform, neglecting small pressure drops.

Initially, condensing sulfur was tried since the condensing temperature of sulfur is close to the maximum temperatures expected in the actual installation. It was found that with a simply built apparatus a uniform temperature tube was difficult to obtain. There were large axial temperature variations, and the tube temperature changed with the shield temperature.

Condensing steam was then tried and found to produce a uniform tube temperature that remained constant when the shield temperature was varied over a wide range. The temperature of the tube was much lower than those expected in the actual installation, but the results were felt to be significant since it is the relative temperature between the tube and shield that is of primary importance.

A schematic diagram of the mock-up is given in Fig. 27. Water vapor rises through the nickel tube and is exhausted to the air. Six thermocouples are bound to the tubing in the same manner as on the actual apparatus, with fiberglass insulation and a thin piece of mica between each thermocouple and the tube. In addition there is one thermocouple silver soldered to the tube for the determination of the true tube temperature. The copper shield has three thermocouples silver soldered to it, and approximately 20 feet of #24 fiberglass insulated chromel wire is wrapped around it for resistance heating. The tube and the shield are both inside a large ceramic tube which acts as a separator of the two steel end supports. A ceramic tube of the same dimensions is used on the actual installation and it was included here to determine its effect on the apparatus operation. The only effect of the ceramic tube was to increase the time for the system to reach equilibrium. This time was appreciably shortened by machining four 1/2 in. holes at the top and bottom and allowing air to circulate between ceramic and copper shield.

The results of the tests run on the mock-up are plotted in Fig. 28. They lead to the following conclusions:

1. The shield temperatures can vary 10°F above or below the actual tube wall temperature and give an accuracy of 1°F on the tube wall temperature reading.

2. The axial temperature distribution of the shield was uniform to within 2°F at all the tested temperature, giving rise to the hope that it would be uniform at higher levels of temperature.

3. The time increments necessary for the apparatus to come to equilibrium, with the shield and tube temperatures the same, was about 10 minutes. This amount of time was not considered unduly long, since in the actual installation, the time necessary to come to equilibrium after a change in operating conditions would certainly be greater then the time to bring the shield to the proper temperature.

Data obtained is given on the next page.

Data

Shield Volts	0	24	30	34	36
Shield Amps	0	2	2.5	2.8	2.0
t_t (^oF)	211.4	211.4	212.0	211.7	212.0
t_1	207.2	209.6	211.1	211.4	212.0
t_2	206.9	209.6	211.1	211.4	212.3
t_3	209.3	210.5	211.4	211.7	212.3
t_4	208.4	210.2	211.4	211.7	212.3
t_5	207.5	209.9	211.4	211.7	212.3
t_6	208.4	210.2	211.4	211.7	212.3
t_{sh1}	147	181	199	209.9	215.6
t_{sh2}	147	182	200	211.1	217.4
t_{sh3}	147	181	200	210.8	217.1
t_t-t_1	4.2	1.8	.9	.3	0
t_t-t_2	4.5	1.8	.9	.3	-.3
t_t-t_3	2.1	.9	.6	0	-.3
t_t-t_4	3.0	1.2	.6	0	-.3
t_t-t_5	3.9	1.5	.6	0	-.3
t_t-t_6	3.0	1.2	.6	0	-.3
t_t-t_{sh}	63	29	12	1	-5.5

APPENDIX D

DISMANTLING OF HAYWARD-TYLER PUMP

Under the supervision of Mr. W. N. Woodard of the DeLaval Steam Turbine Co., the Hayward-Tyler pump was completely dismantled, except for the upper motor assembly. Figs. 29 through 35 are photographs of the pump, recording the work as it progressed.

Fig. 29 shows the pump as it was removed from the test cell. Fig. 30 shows the pump housing which contained a pool of rusty, oily water. It might be noted that because of the height of the inlet and outlet ports above the bottom of the pump housing, a quantity of water always remains at the bottom, making the task of completely flushing quite difficult.

Fig. 31 was taken with the pump assembly removed for inspection and cleaning. Fig. 32 is the entire four-stage pump assembly as it is contained in the pump, and Fig. 33 is a blown-up view of the bottom stage of the pump assembly, the right side being the bottom. Reading from left to right the parts are: pump impeller, guide vanes, wearing plate, split ring, return vanes, wearing plate, split ring, and pump bearing housing.

Fig. 34 is a close-up of the guide vanes and impeller and shows clearly the poor quality of the stainless steel castings, which contained blowholes and imbedded sand particles. The fact that the impeller blades were not machined is perhaps one of the major factors causing such low pump efficiencies (Cf.Fig.8).

The shaft as seen in Fig. 31 was checked with a dial indicator and a run-out of .014 in. Total Indicator Reading was found. The cause of the run-out could not be determined. This run-out may, or may not, be objectionable, but might increase the danger of galling at the wearing rings. The total wearing ring clearance was .005 in. It was at these points that the pump at U.C.L.A. galled, necessitating increasing the clearance to .010 in.

The entire pump assembly was washed in a solution of Oakite and wire brushed in an attempt to remove deposited rust and some of the imbedded sand. The first was successful but little sand was removed. It was feared at that time that this sand might dislodge at high water temperatures and be carried around through the system. No particles of sand have ever been found but chemical analysis has shown SiO_2 to be present in the test water.

The pump assembly was put back into place, and the motor casing removed. Fig. 35 shows the motor stator which was covered with a heavy coating of rust. This was washed off and the casing reassembled. No further disassembly was done for fear of disturbing the Kingsbury thrust bearing located at the top. This bearing carries the entire weight of the motor rotor, shafting, and pump assembly.

The pump was then given a hydraulic pressure test of approximately 4000 psig, which was retained for about two hours with no visible leaks or drop in pressure.

REFERENCES

1. Osborn, P. W., and Somma, E. H., Heat Transfer at High Rates to Water Flowing in Tubes with Surface Boiling, S. M. Thesis, Dept. Mech. Eng., M. I. T., May 1950.

2. Barton, W. W., Design of Test Equipment for a Study of Surface Boiling of Water, S. M. Thesis, Dept. Mech. Eng. M. I. T., May 1949; Progress Report No. 2, D.I.C. Project 6627, M. I. T, May 10, 1949.

3. Kreith, F. and Summerfield, M., Investigation of Heat Transfer at High Heat Flux Densities: Experimental Study with Water of Friction Drop and Forced Convection with and without Surface Boiling in Tubes, Progress Report No. 4-68, Jet Propulsion Lab., C. I. T., 1948.

4. McAdams, W. H., Kennel, W. E., Minden, C. S., Carl, R., Picornell, P. M., and Dew, J. E., Heat Transfer at High Rates to Water with Surface Boiling, Industrial and Engineering Chemistry, Vol. 41, Pg. 1945, Sept. 1949.

5. Rohsenow, W. M., and Clark, J. A., Progress Report No. 5, D. I. C. Project 6627, M. I. T., June 1, 1950

6. Tables of Thermocouple Characteristics, General Electric Publication GET-1415

LAYOUT OF TEST APPARATUS

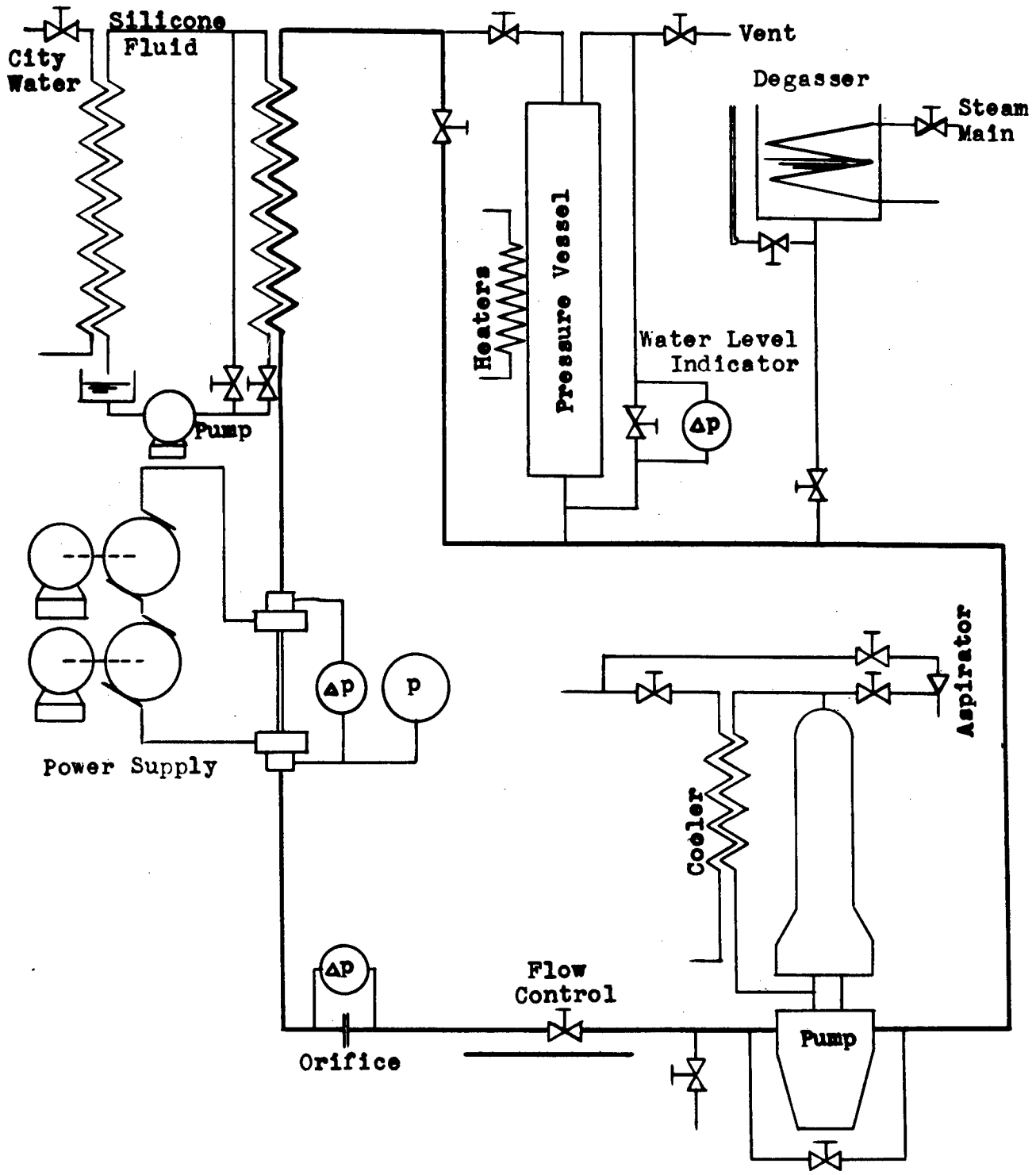

PVO
EHS
4/20/50

Fig. 1

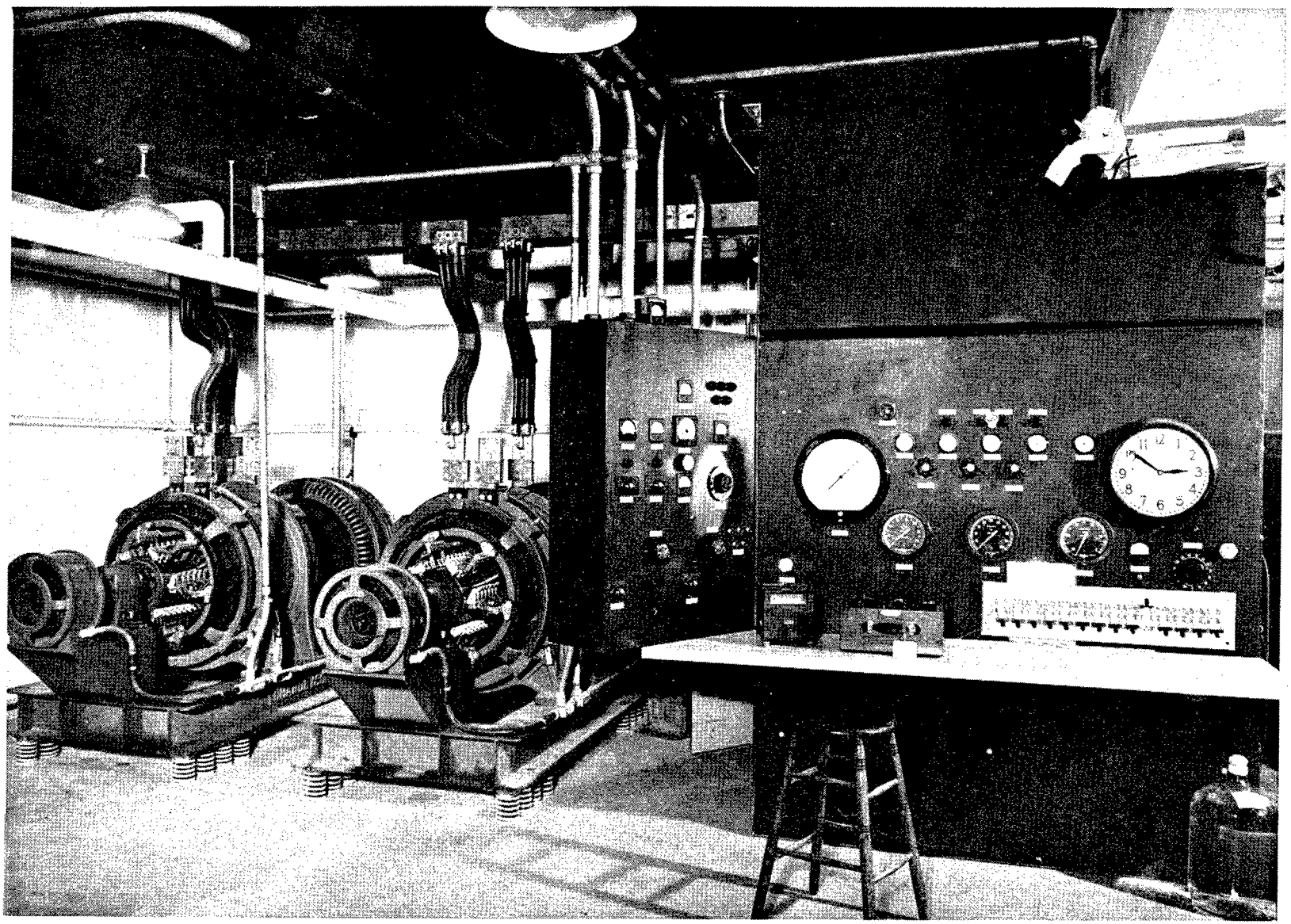

Fig. 2

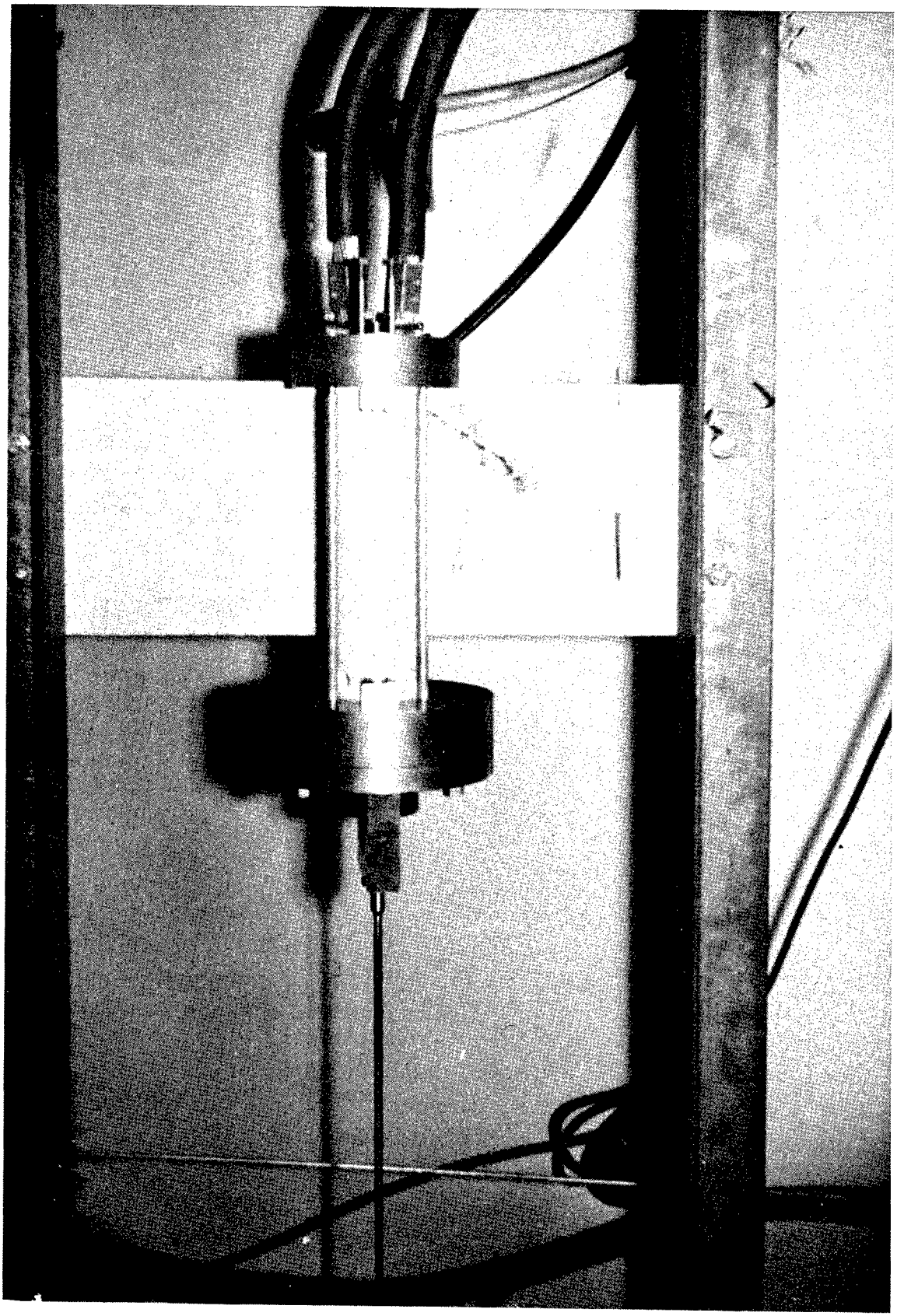

Fig. 3

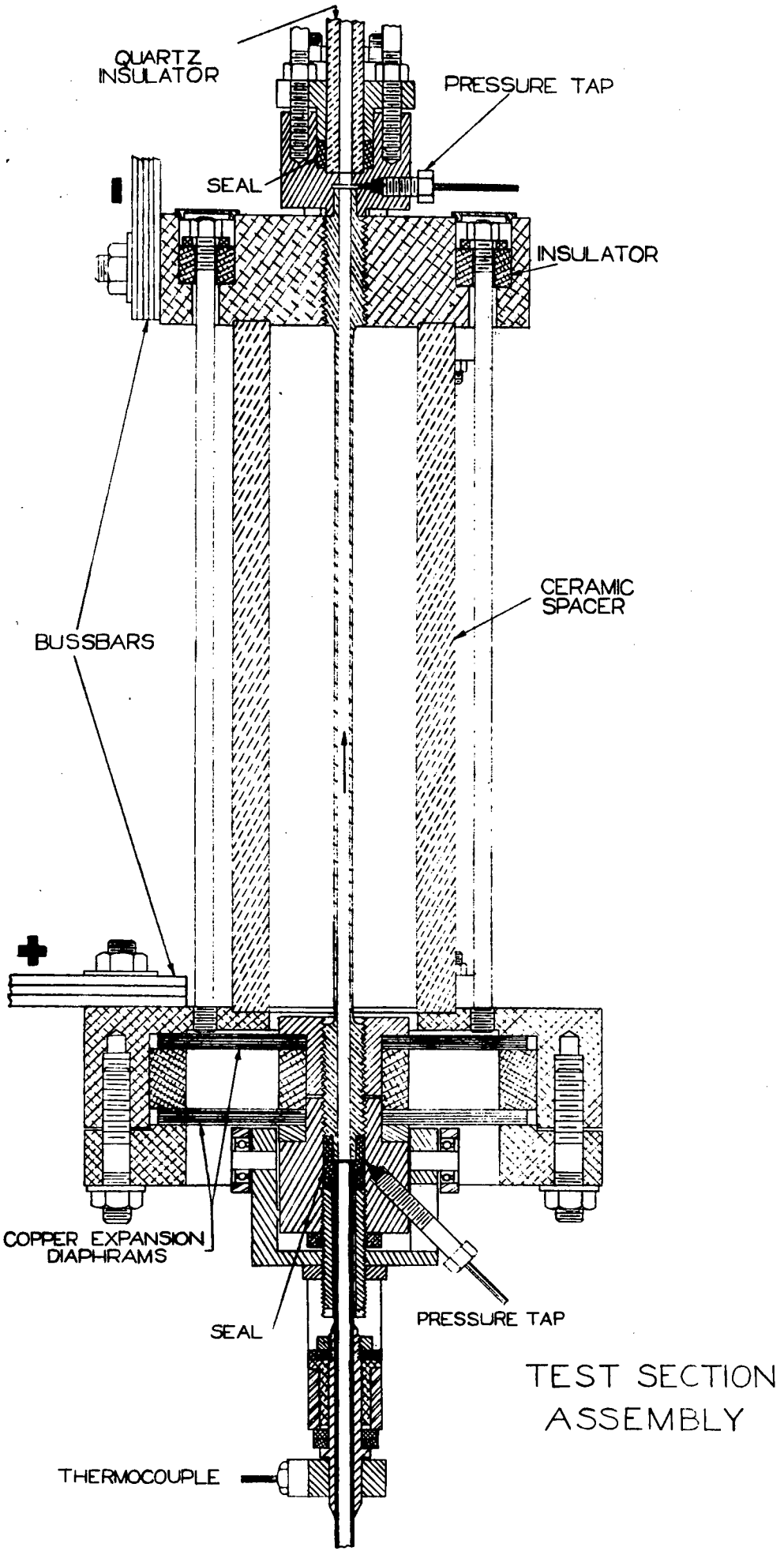
QUARTZ INSULATOR
PRESSURE TAP
SEAL
INSULATOR
CERAMIC SPACER
BUSSBARS
COPPER EXPANSION DIAPHRAMS
SEAL
PRESSURE TAP
THERMOCOUPLE
TEST SECTION ASSEMBLY

Fig. 4

WIRING DIAGRAM GENERATOR #1

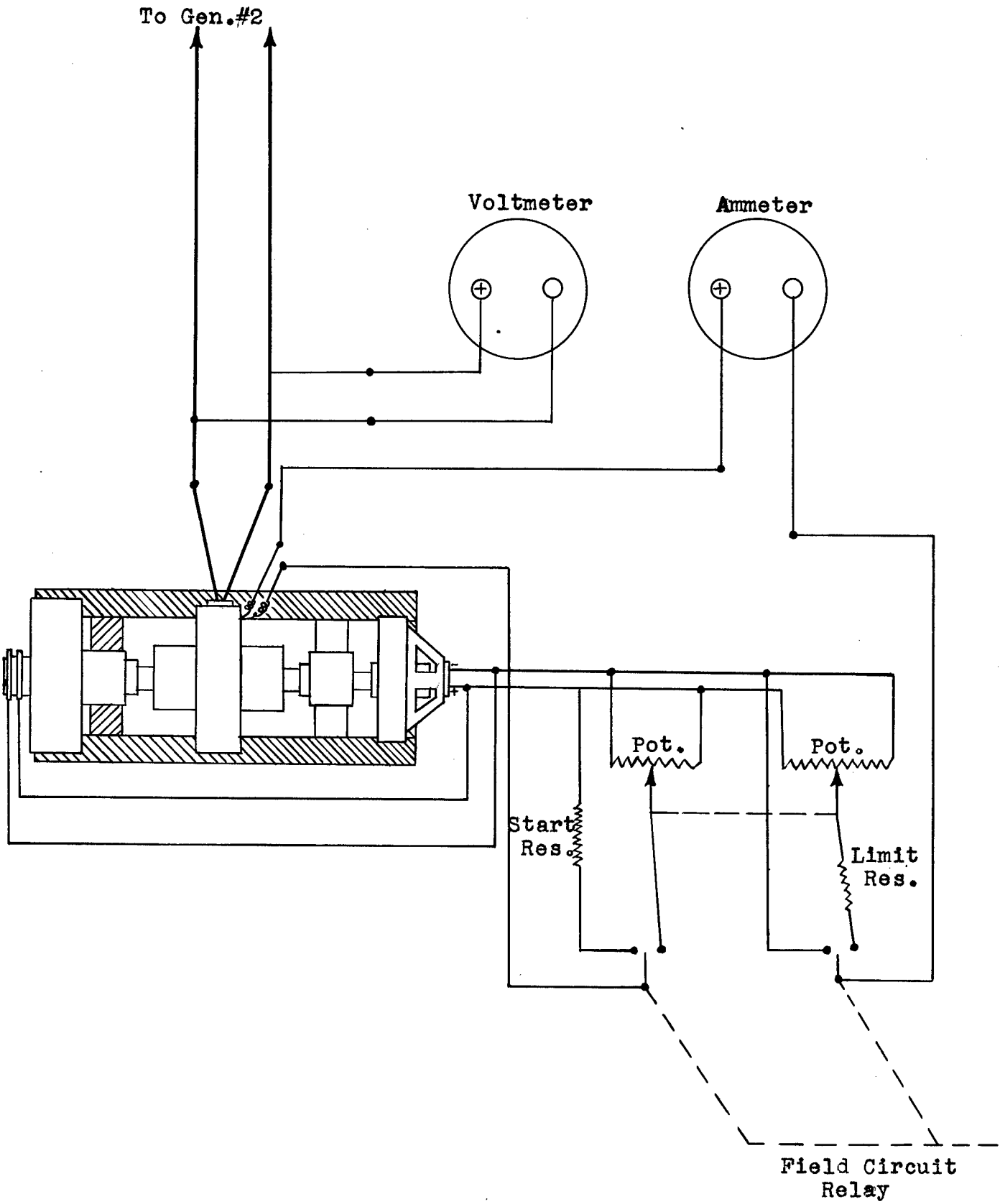

Fig. 5

WIRING DIAGRAM GENERATOR #2

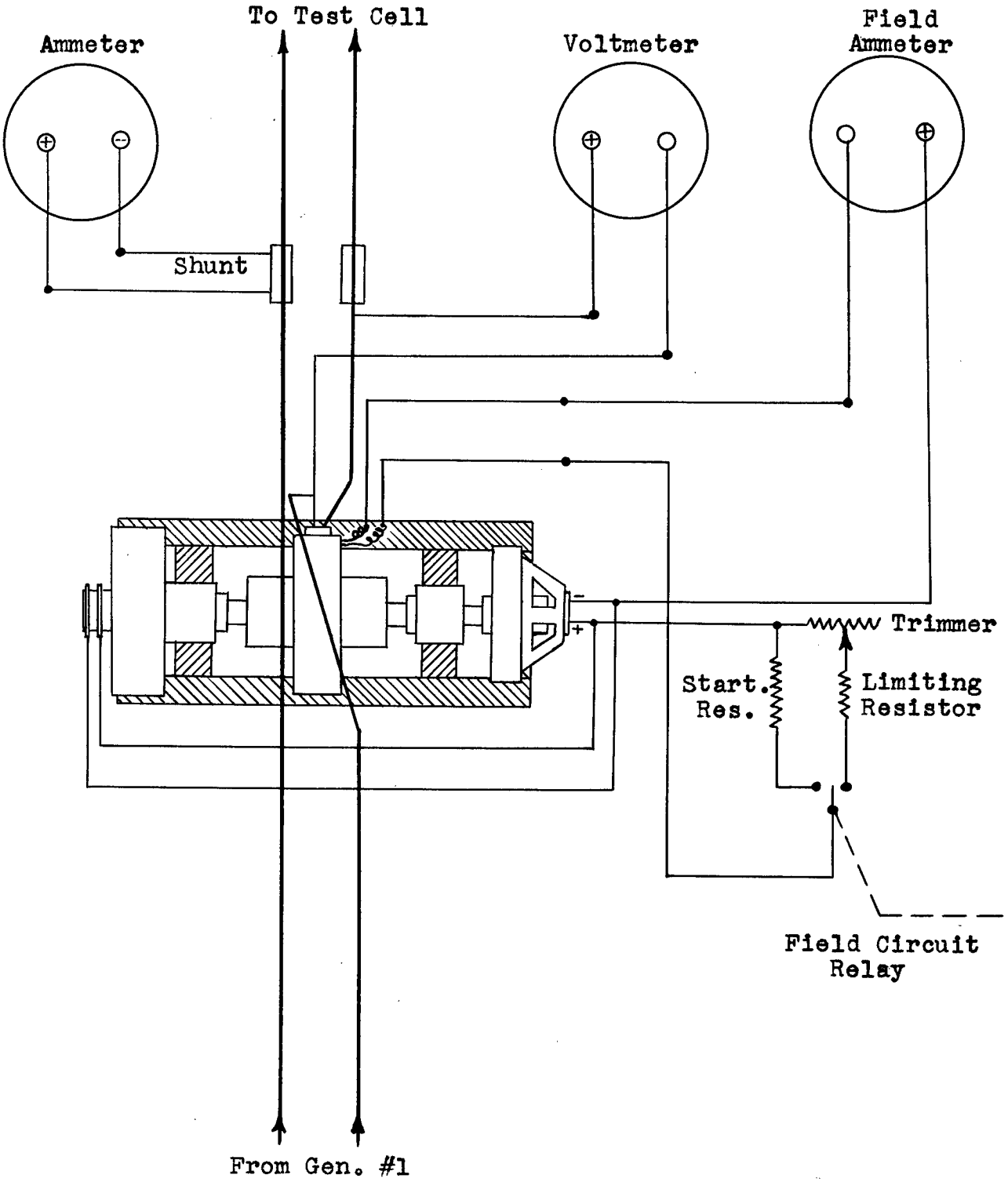

Fig. 6

DD-9480

SENT TO DELAVAL CO. - CHICAGO, ILLINOIS
SUBJECT ARGONNE NATIONAL LABORATORY
BAILEY ROAD, DUPAGE COUNTY, ILL.

OUR ORDER NO 252892
CUST ORDER NO AL-32200 (CR-48716)

WHEN ENDORSED HERE SIGNS ARE CORRECT FOR CONSTRUCTION SUBJECT TO MANUFACTURING TOLERANCES. PRINT IS LOANED SUBJECT TO RETURN UPON DEMAND AND UPON THE EXPRESS CONDITION THAT IT IS NOT TO BE USED DIRECTLY OR INDIRECTLY IN ANY WAY DETRIMENTAL TO OUR INTERESTS

DE LAVAL STEAM TURBINE CO.
TRENTON, NEW JERSEY

ENDORSED BY [signature]
ASSISTANT ENGINEER

DATE 9-14-49

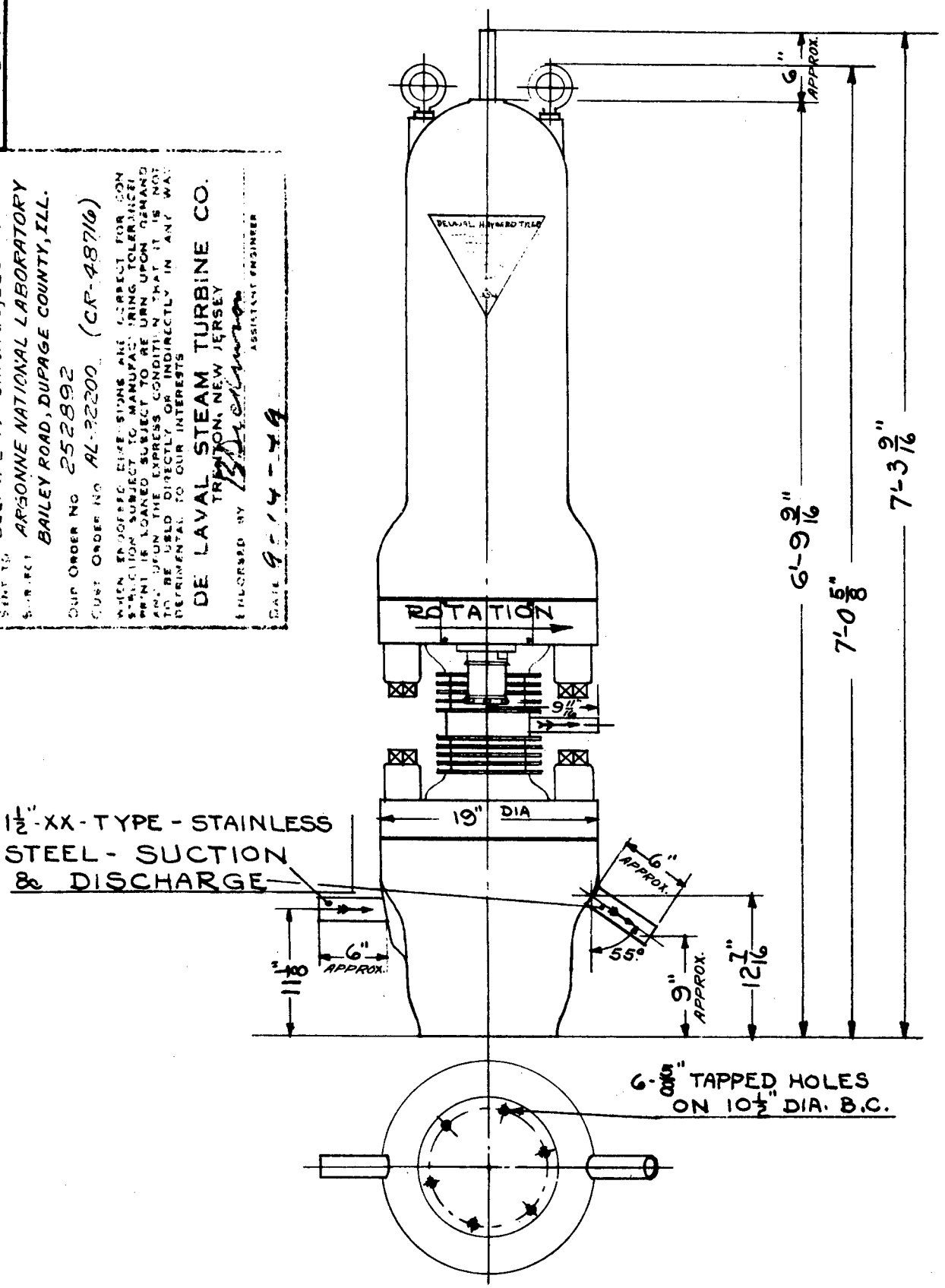

ALT.		DELAVAL STEAM TURBINE CO. TRENTON, N. J.		SCALE
DRAWN BY	ARN	TITLE	ORDER NO	1"=1'-0"
TRACED BY		OUTLINE OF 9 HP. BOILER CIRCULATING PUMP	252982	DATE
APPROVED				9-2-49

DD-9480

222-15

Fig. 7

E D 210-2

CHARACTERISTIC CURVE

SHOWING PERFORMANCE OF

~~TURBINE DRIVEN~~)
MOTOR DRIVEN
~~GASOLINE ENGINE~~) CENTRIFUGAL PUMP

C. C. 60994

FOR ARGONNE NATIONAL LABORATORY

NO. 253010-11 TYPE

AVERAGE SPEED 3550 R. P. M.

SUCTION ~~LIFT~~ + 2 FT.

DATE OF TEST 11-10-49

V. Hawthorne

DE LAVAL STEAM TURBINE CO.
TRENTON, N. J.

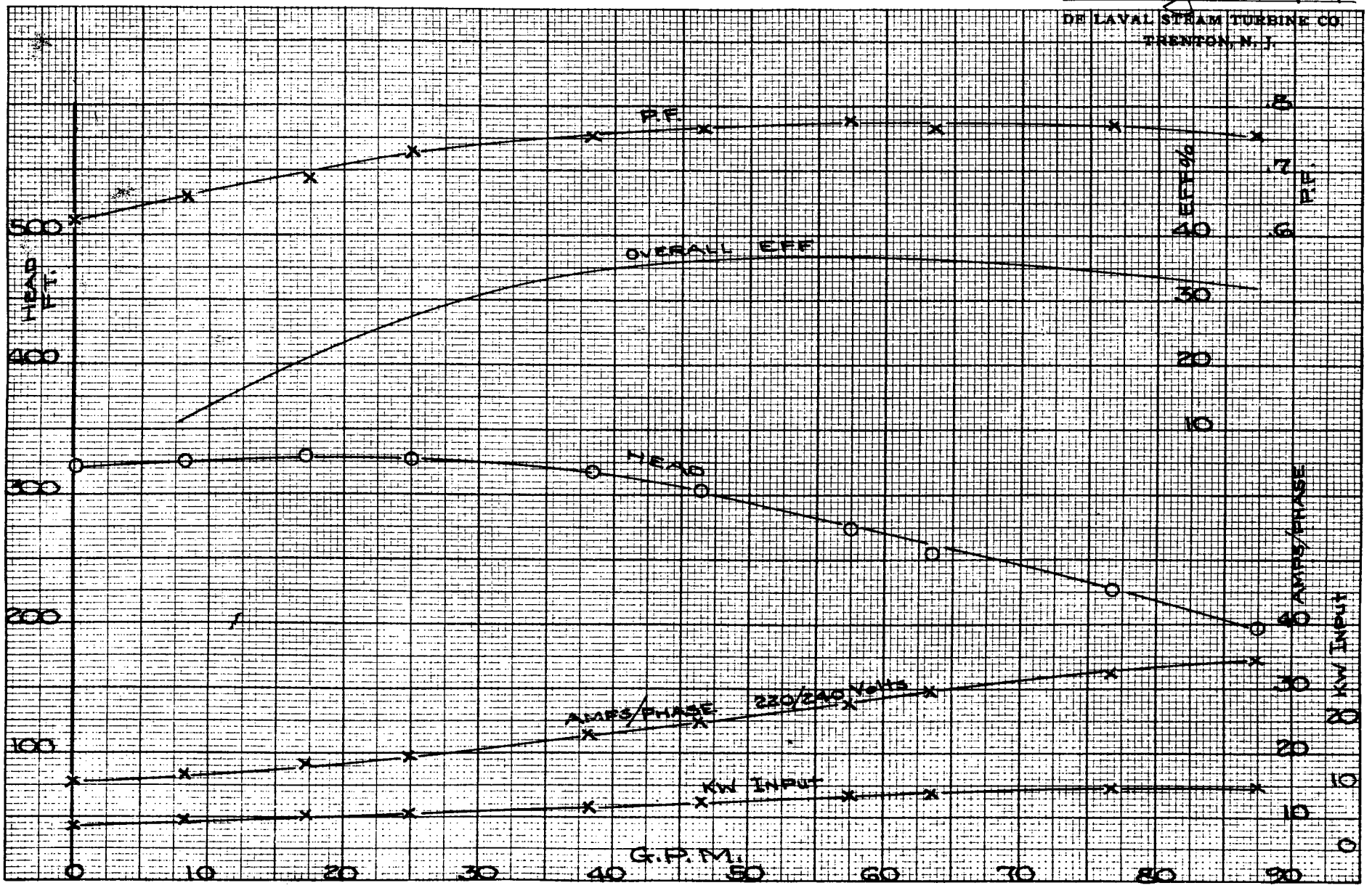

Fig. 8

LAYOUT OF HEAT EXCHANGERS

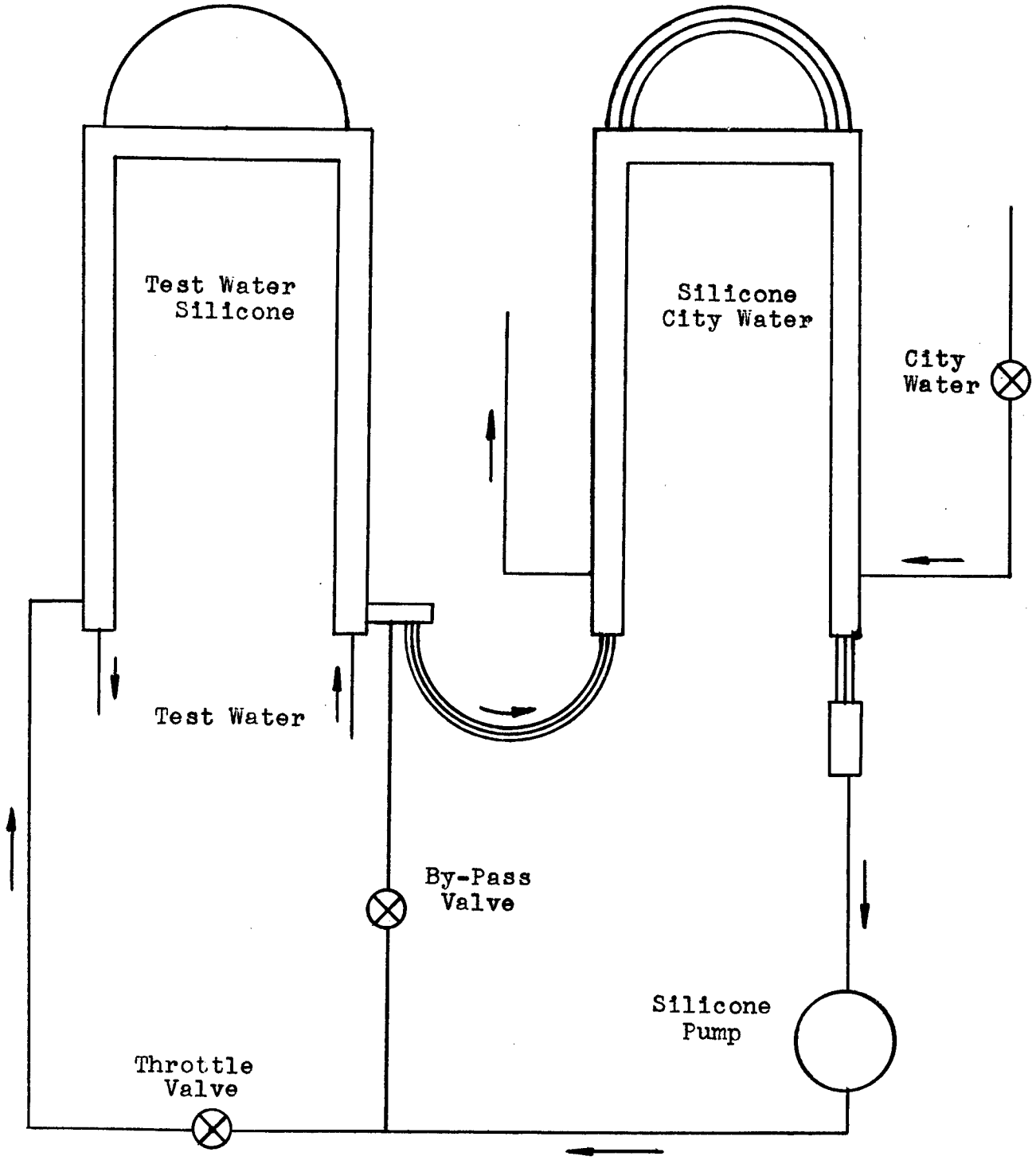

PVO
EHS
4/20/50

Fig. 9

LAYOUT OF PRESSURE VESSEL

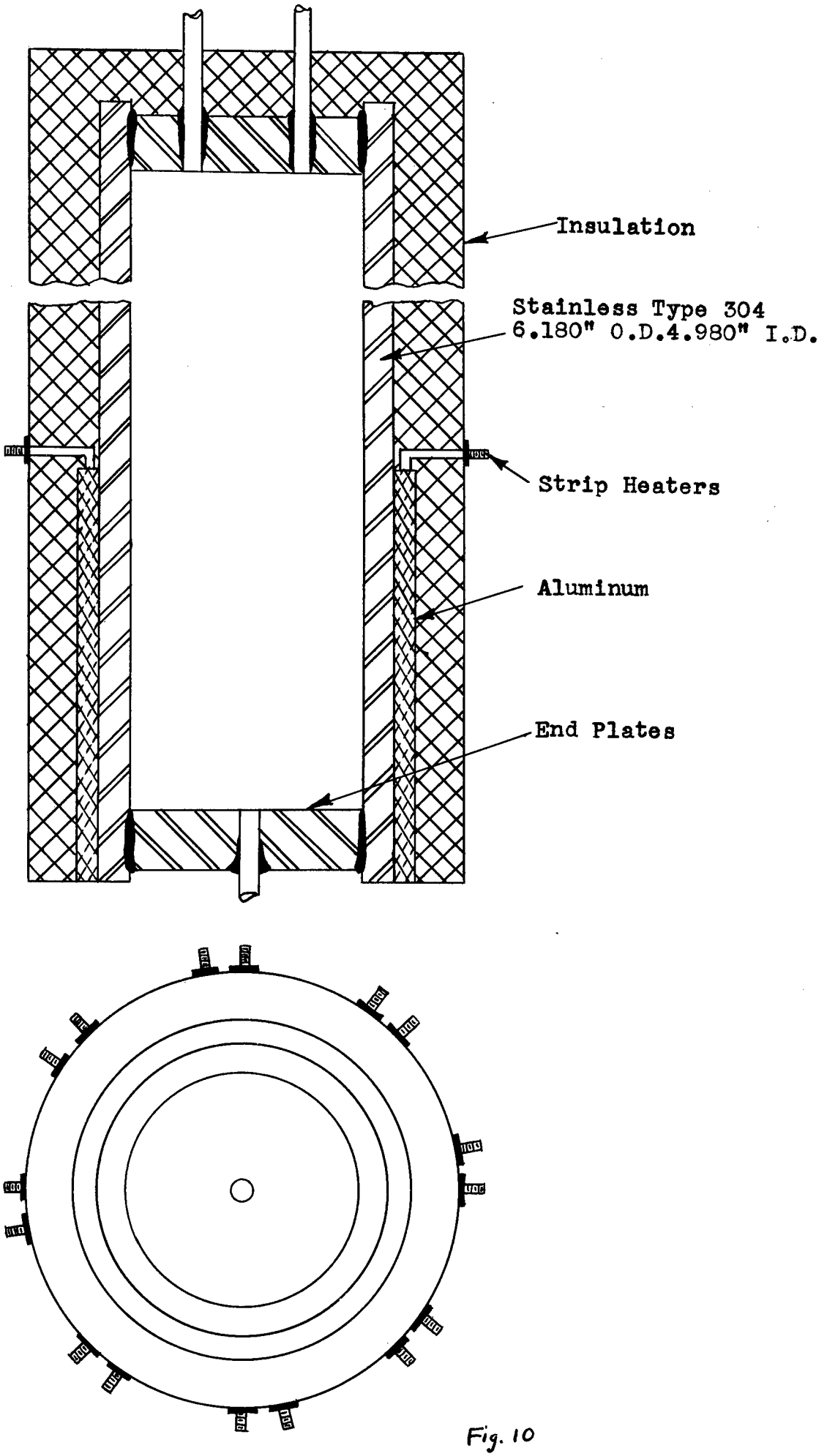

Fig. 10

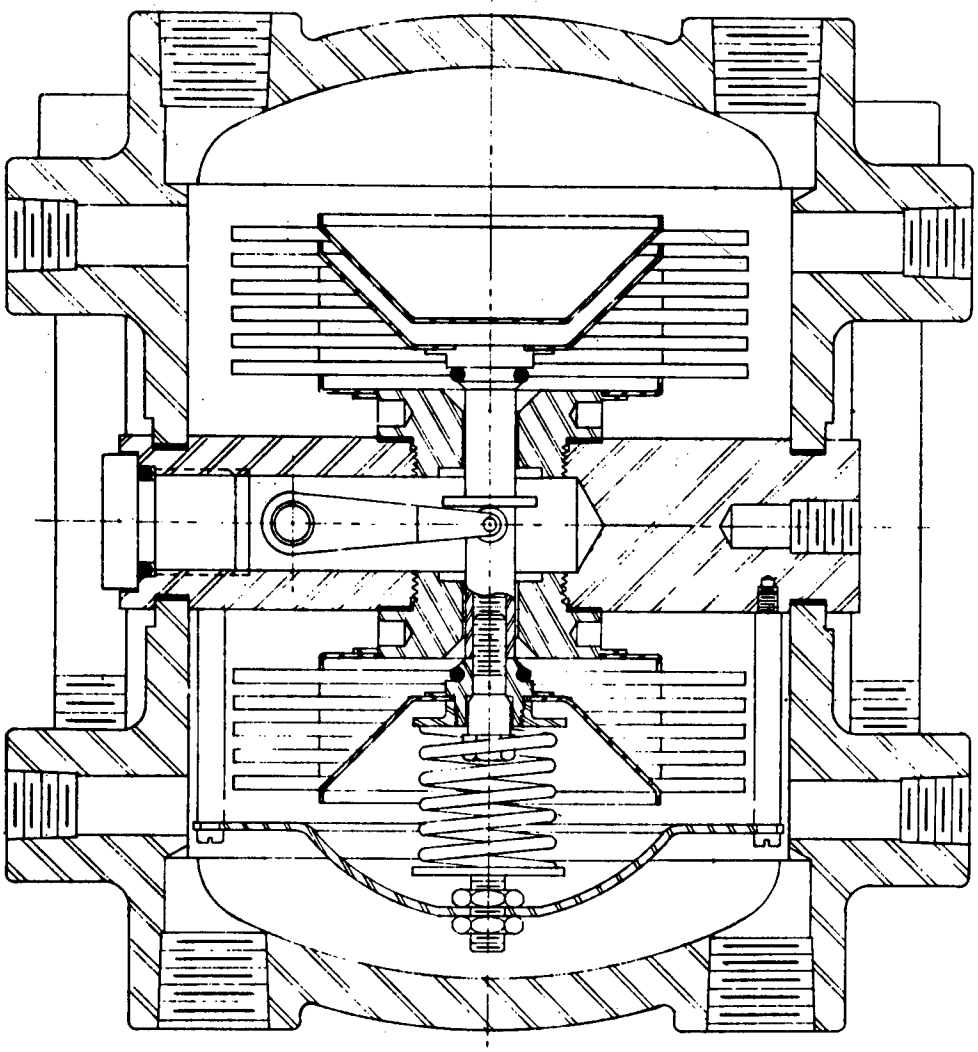

Patent No. 2400048
Other Patents Pend.

Fig. 11

MATL.				FINISH	
SCALE Full	DATE 3 Aug 48	DRAWN RBP	CHECKED	ENGR. APPR.	PROD. APPR.
LIMITS ON DIMENSIONS UNLESS OTHERWISE NOTED: ANGULAR ± 1/2° FRACTIONAL ± 1/64 DECIMAL ± .005		SECTIONAL VIEW OF MODEL 199 D.P. UNIT 1500 PSI RATING			
BARTON INSTRUMENT CO.		LOS ANGELES, CALIF.		DWG. NO. DA 199-4	

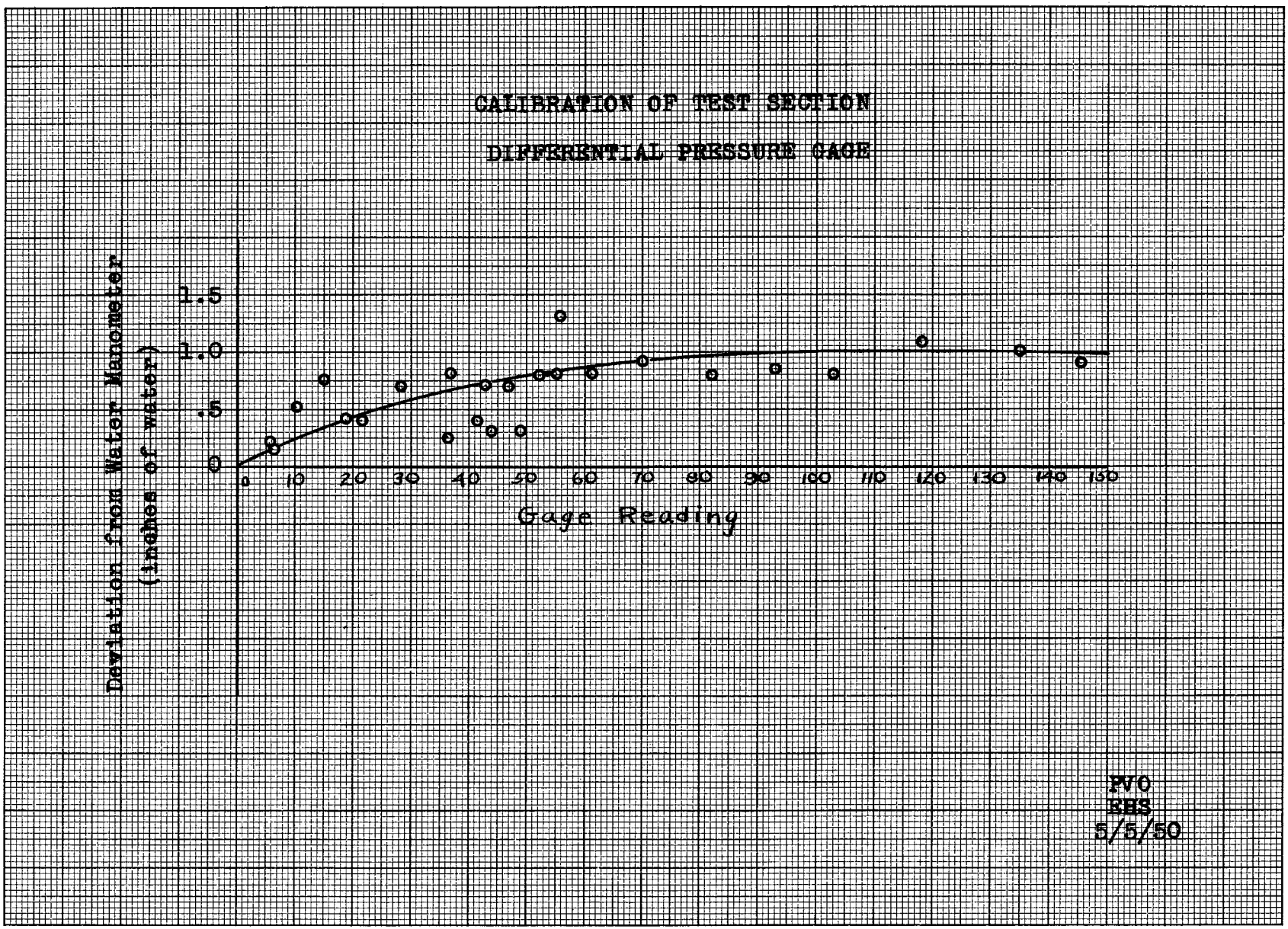
CALIBRATION OF TEST SECTION
DIFFERENTIAL PRESSURE GAGE
Deviation from Water Manometer (inches of water)
1.5
1.0
.5
0
0
10
20
30
40
50
60
70
80
90
100
110
120
130
140
150
Gage Reading
PVO
EBS
5/5/50

Fig.12

PRESSURE VESSEL LIQUID LEVEL INDICATOR

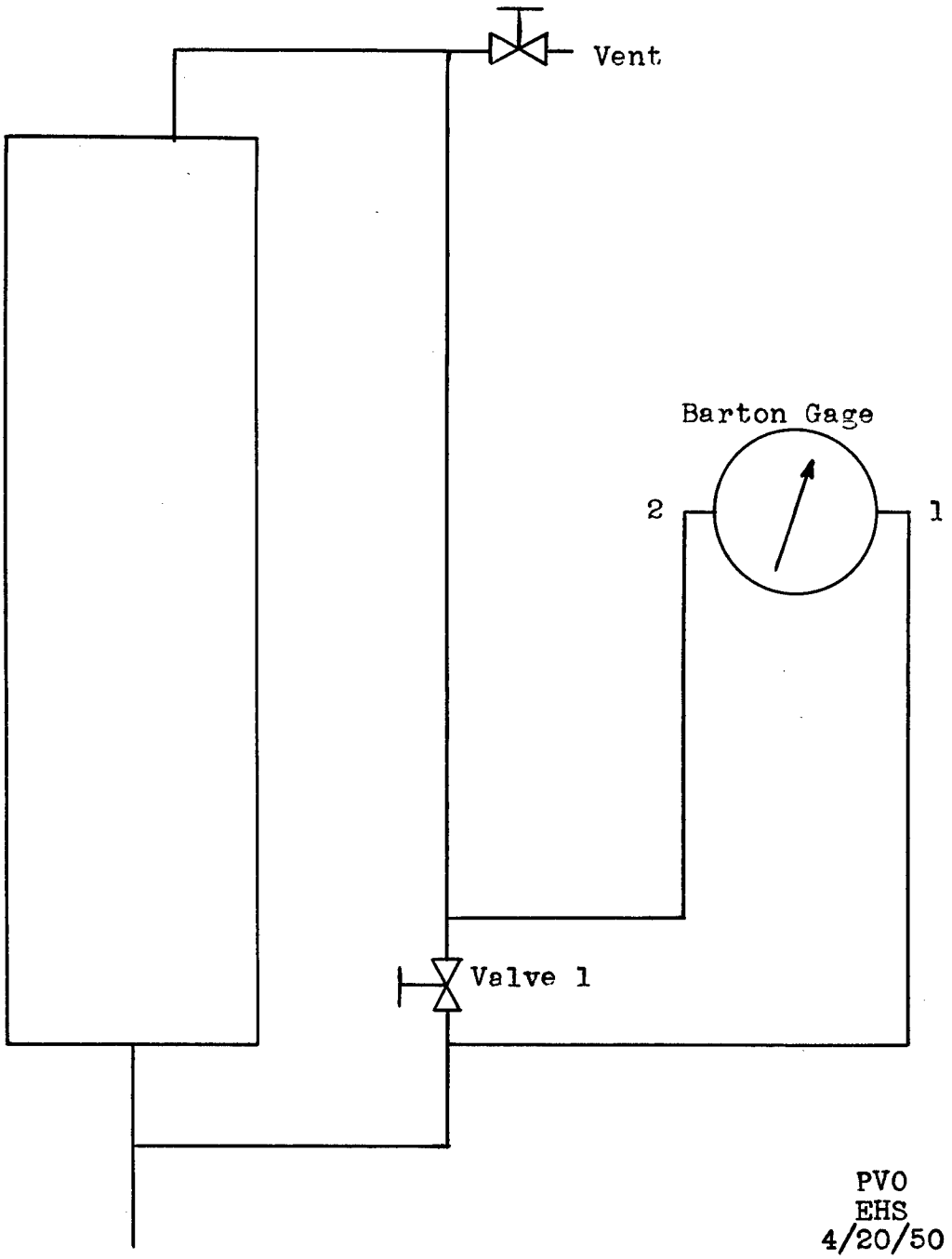

Fig. 13

Form 259
16—41016-1

UNITED STATES DEPARTMENT OF COMMERCE
WASHINGTON

National Bureau of Standards

REPORT

of Test of

CURRENT SHUNT
0.00001667 ohm, for 3000 amperes
General Electric Company, No Serial No.

Submitted by

Massachusetts Institute of Technology
Attn. Mr. Paul V. Osborn, Jr.
Res. Asst. Mech. Eng.
Department of Mechanical Engineering
Cambridge 39, Massachusetts

The resistance of this shunt, when measured on December 6, 1949, after temperature equilibrium had been attained under the conditions specified below, had the following values:

Shunt Temperature °C	Test Current Amperes	Resistance Absolute Ohms
24	600	1.6603×10^{-5}
50	600	1.6632×10^{-5}
75	600	1.6647×10^{-5}
100	600	1.6656×10^{-5}

The values of resistance given above were correct, as of the above date, within 0.1 percent for the condition of the test, i.e. uniform current distribution insured by cleaned copper busbars symmetrically arranged to completely fill the slots, and potential-tap location fixed by inserting insulated washers below the metal washers under the potential-tap screw-heads.

For the Director

F. M. Defandorf

F. M. Defandorf, Chief
Electrical Instruments Section
Division of Electricity and Optics

1.3/123403
Your letter of 11/25/49
December 20, 1949

Fig. 14

TEST SECTION VOLTAGE MEASUREMENT

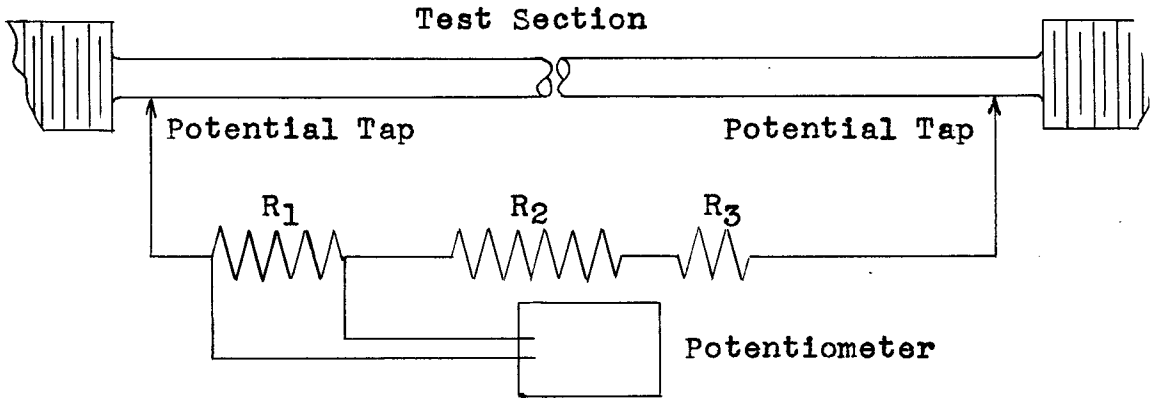

PVO
EHS
4/20/50

Fig. 15

LOCATION OF THERMOCOUPLES AND POTENTIAL TAPS

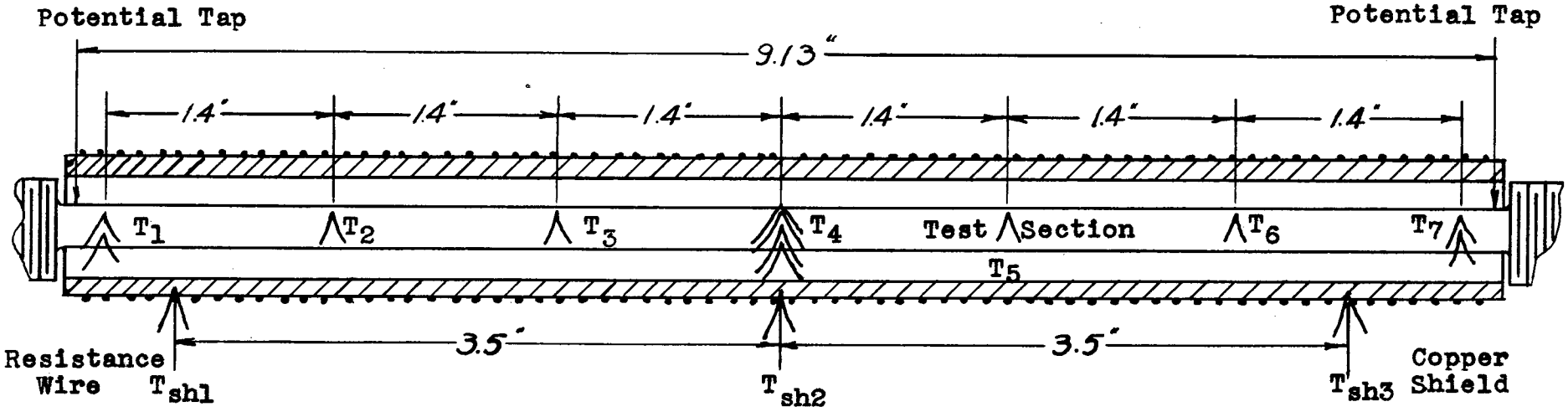

PVO
EHS
4/20/50

Fig. 16

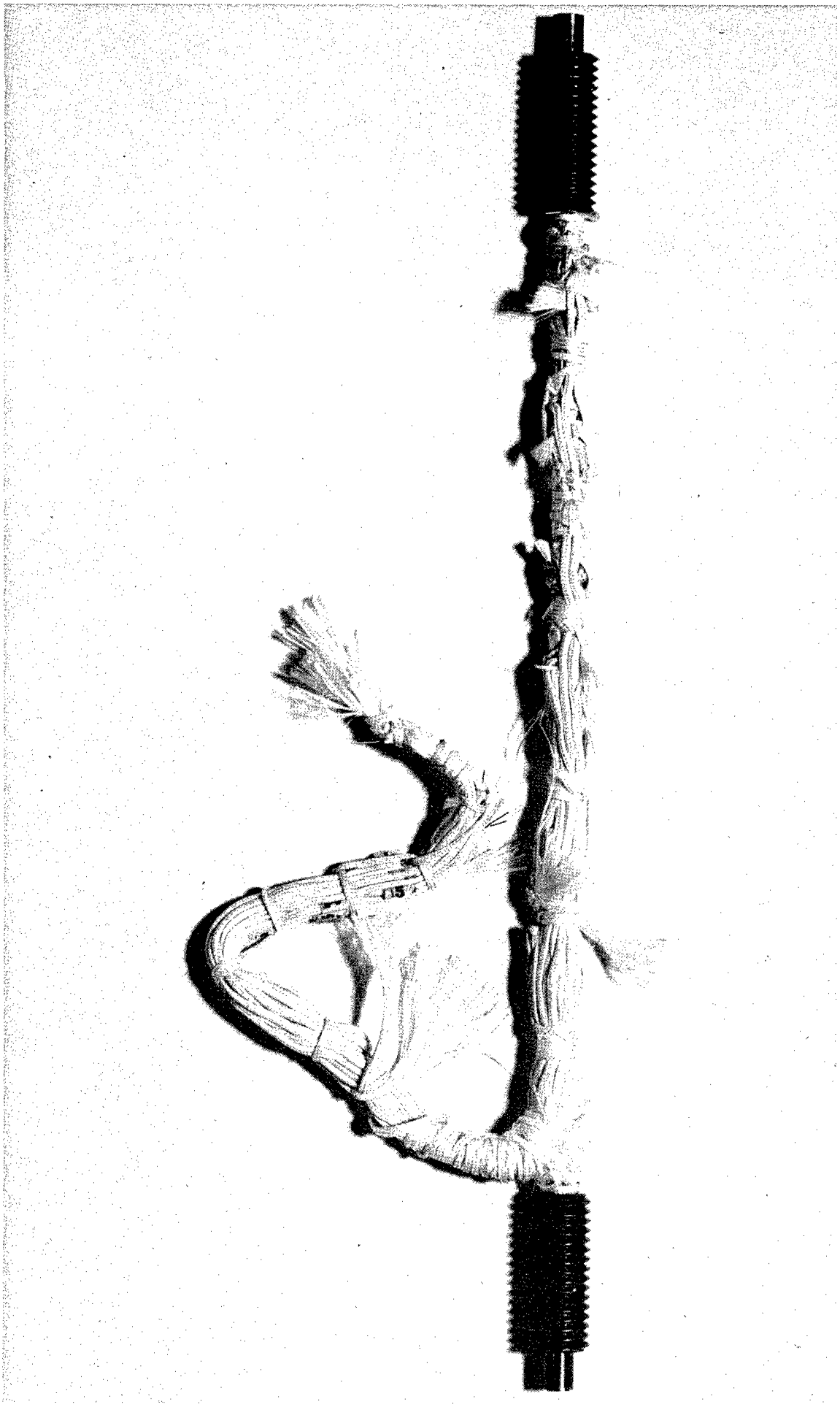

Fig. 17

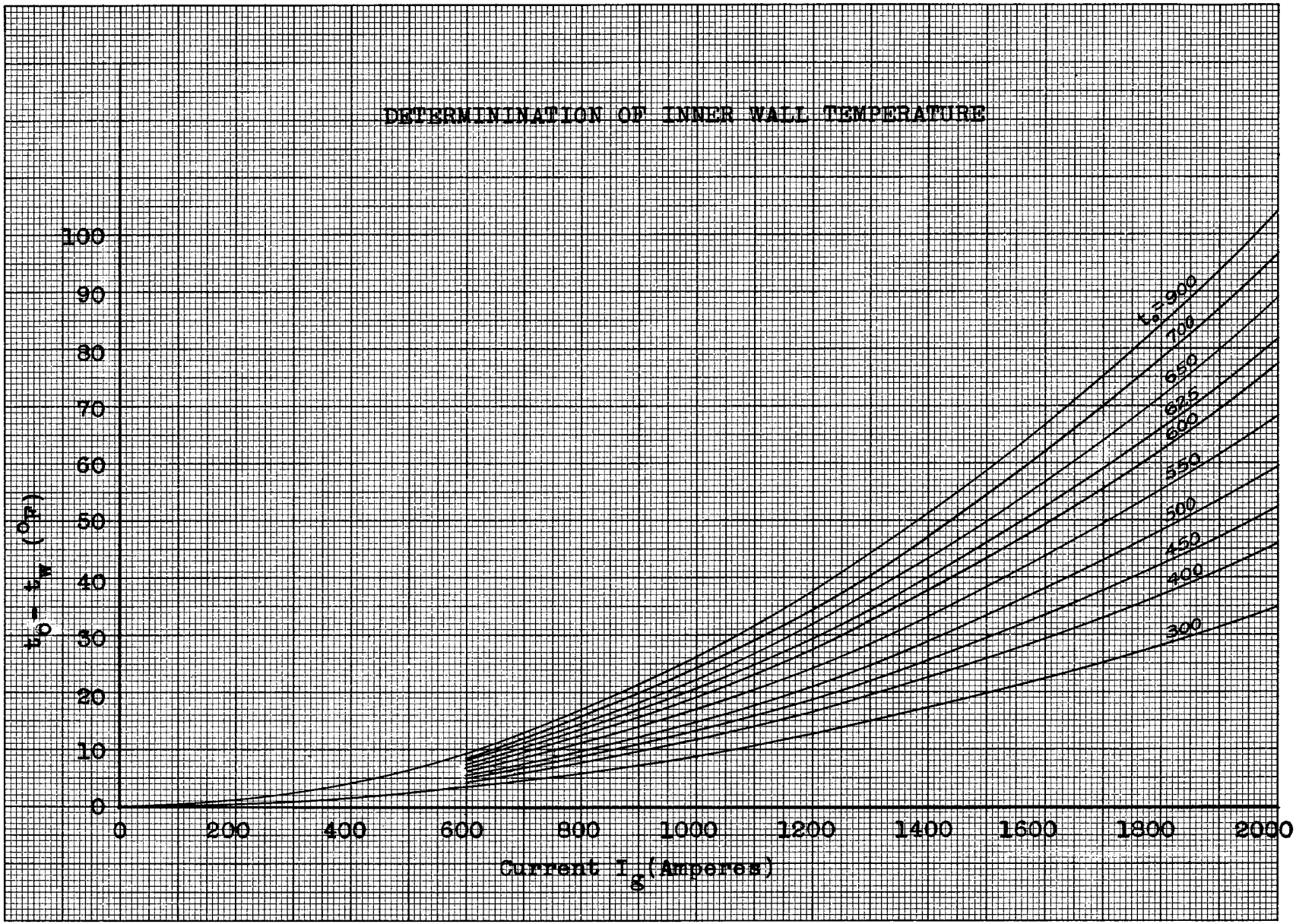

Fig. 18

PVO
EHS
5/3/50

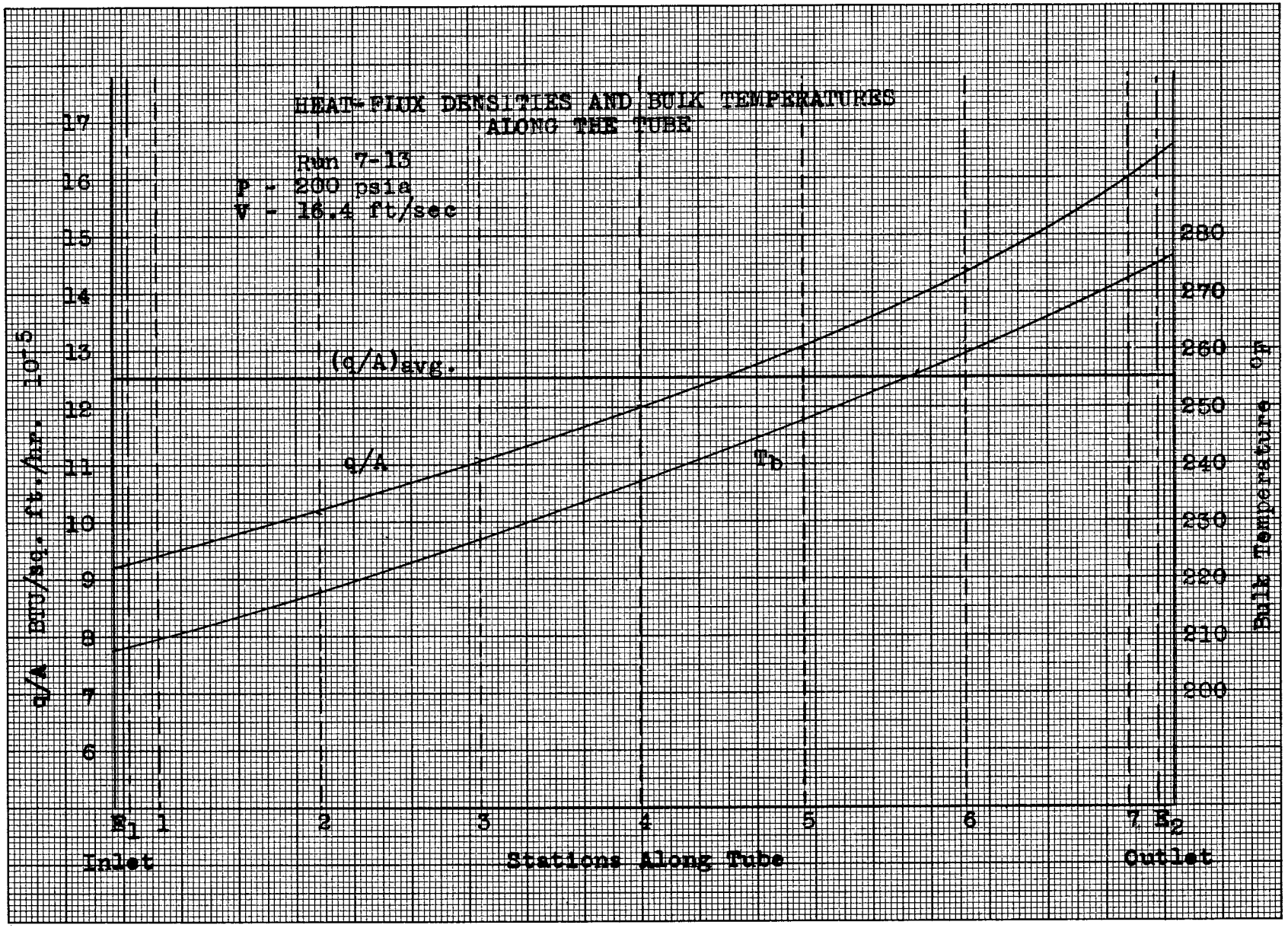

Fig. 19

PVO
EHS
5/8/50

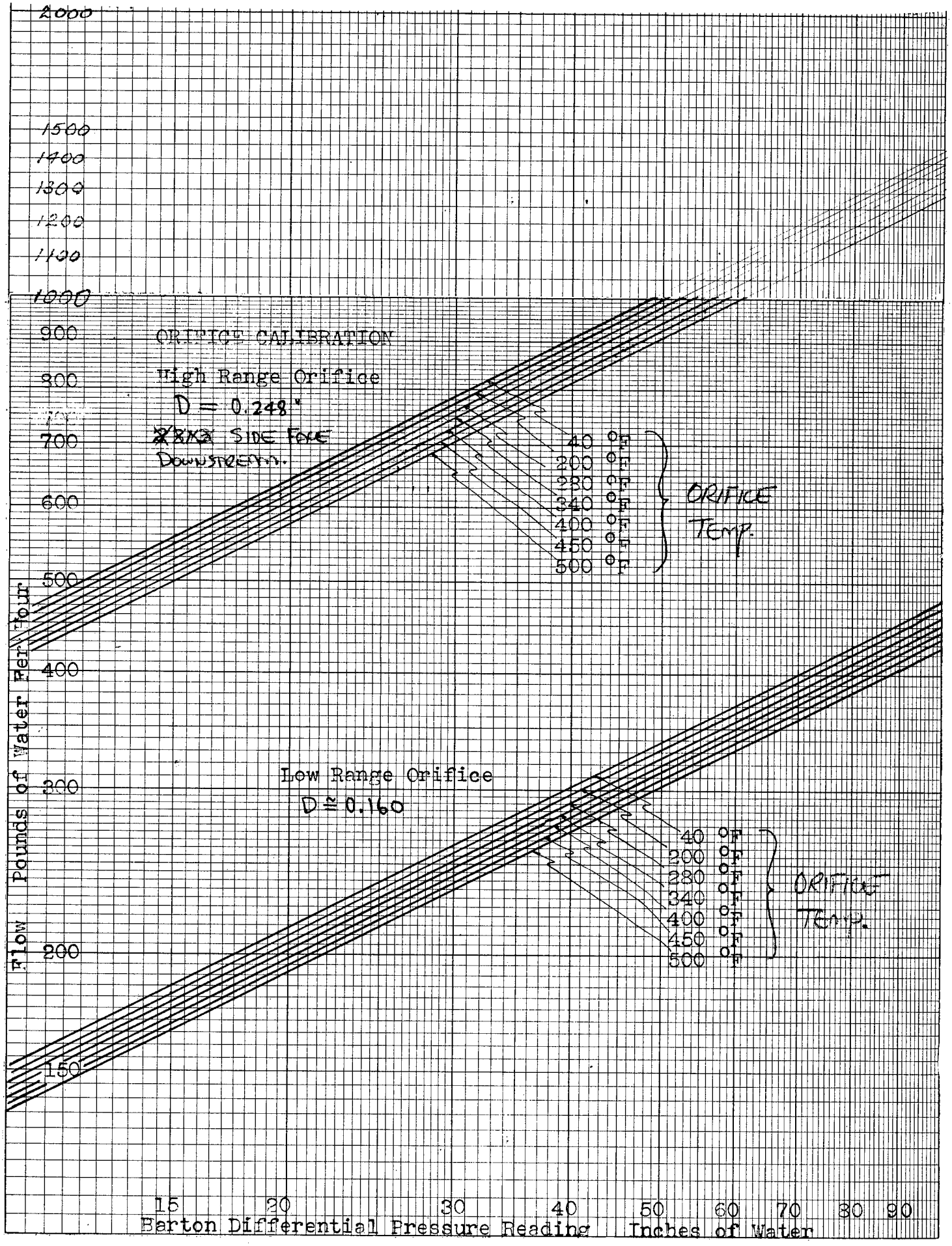
ORIFICE CALIBRATION
High Range Orifice
D = 0.248"
SIDE FACE
DOWNSTREAM.
40 °F
200 °F
280 °F
340 °F
400 °F
450 °F
500 °F
ORIFICE TEMP.
Low Range Orifice
D = 0.160
40 °F
200 °F
280 °F
340 °F
400 °F
450 °F
500 °F
ORIFICE TEMP.
Flow Pounds of Water Per Hour
2000
1500
1400
1300
1200
1100
1000
900
800
700
600
500
400
300
200
150
15
20
30
40
50
60
70
80
90
Barton Differential Pressure Reading Inches of Water

Fig. 20

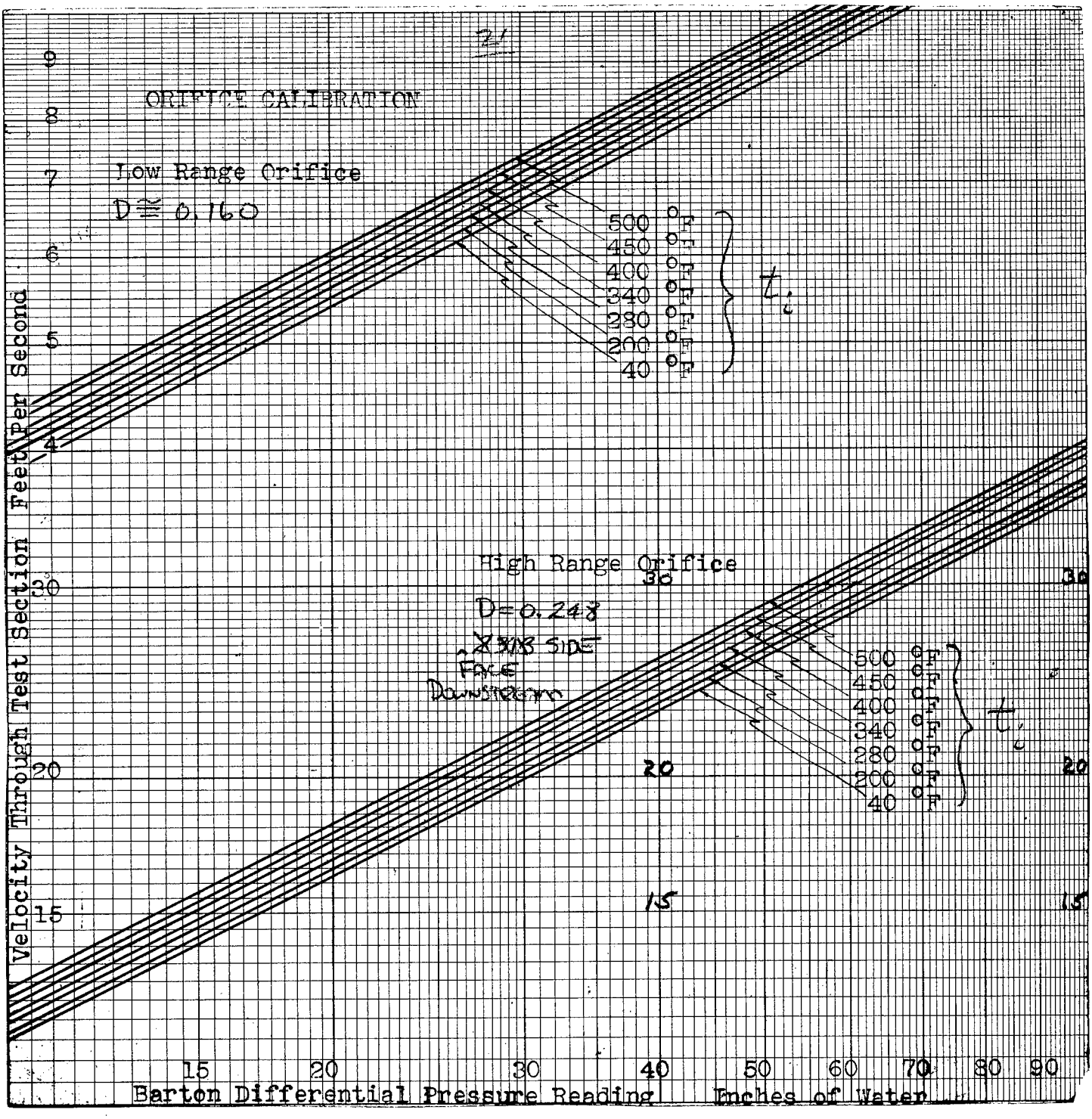
21
ORIFICE CALIBRATION
Low Range Orifice
D = 0.160
500 °F
450 °F
400 °F
340 °F
280 °F
200 °F
40 °F
t_c
High Range Orifice
D = 0.248
Sharp Side Face Downstream
500 °F
450 °F
400 °F
340 °F
280 °F
200 °F
40 °F
t_c
Velocity Through Test Section Feet Per Second
Barton Differential Pressure Reading Inches of Water
9
8
7
6
5
4
30
20
15
15
20
30
40
50
60
70
80
90

Fig. 21

NICKEL RESISTIVITY MEASURING APPARATUS

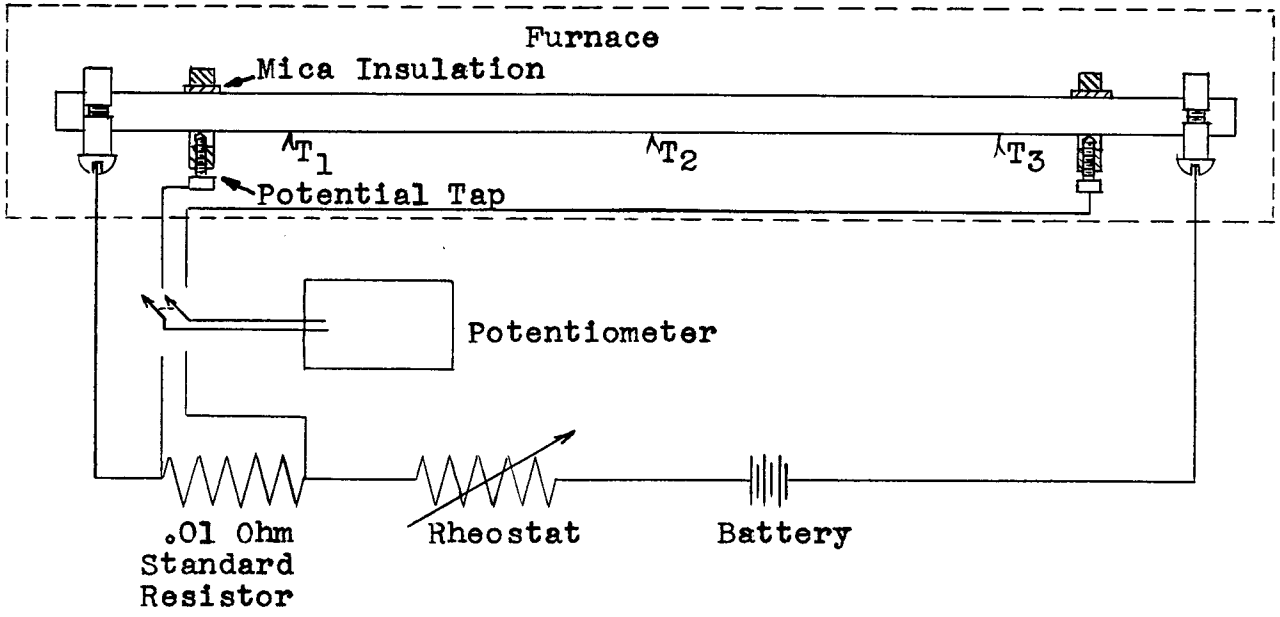

Fig.22

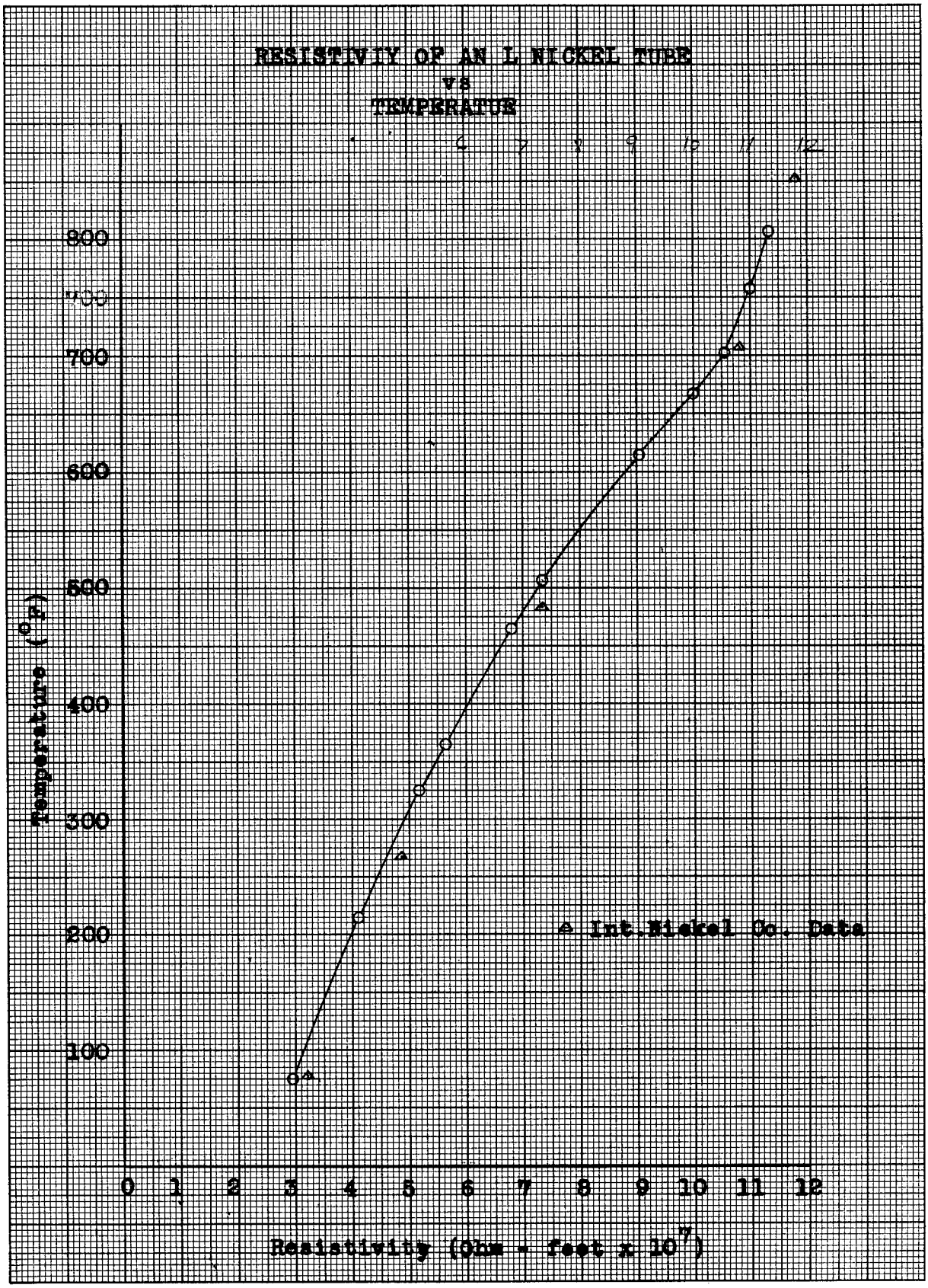

PVO
EHS
4/16/50

Fig.23

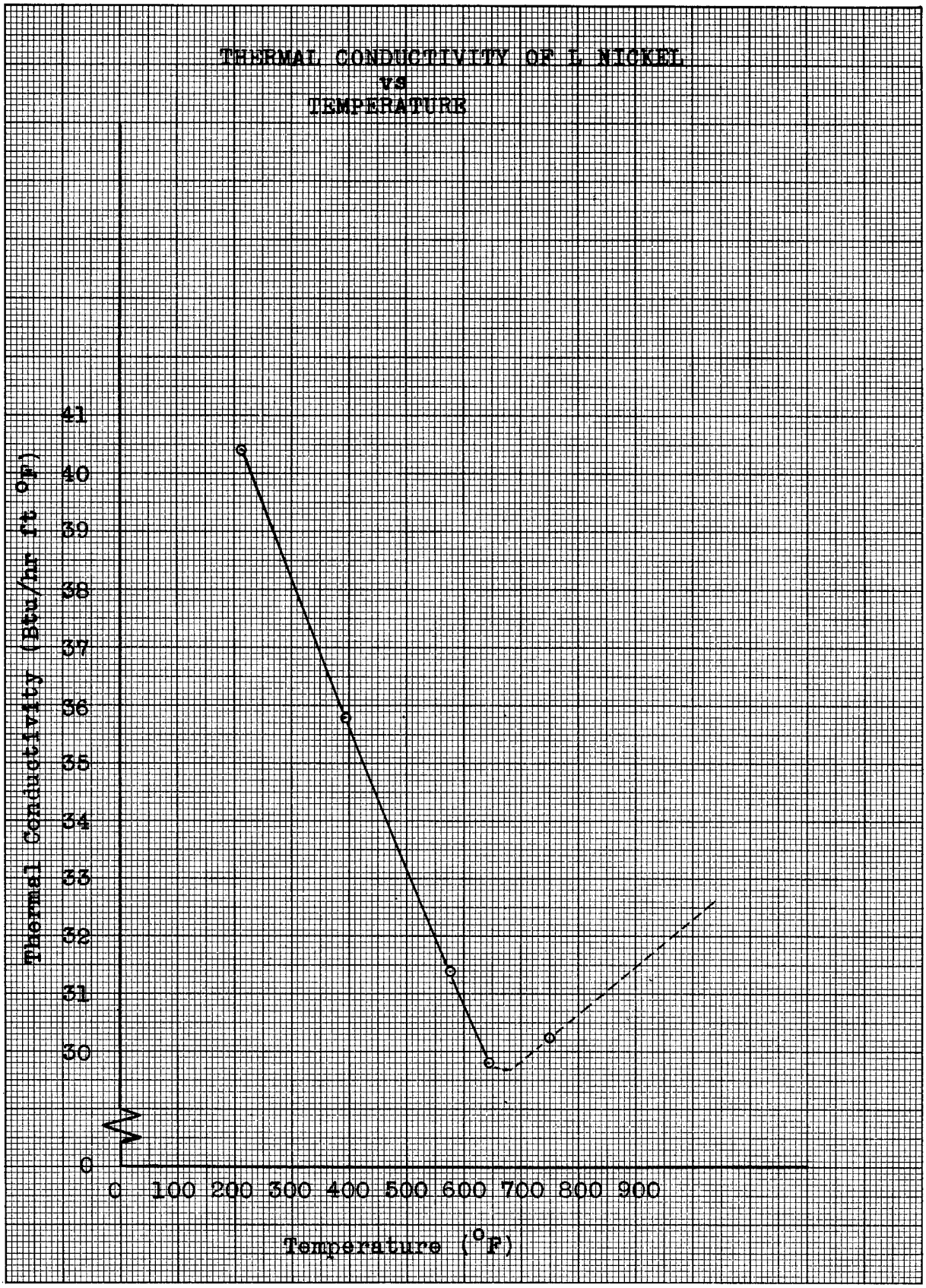

PVO
EHS
4/16/50

Fig. 24

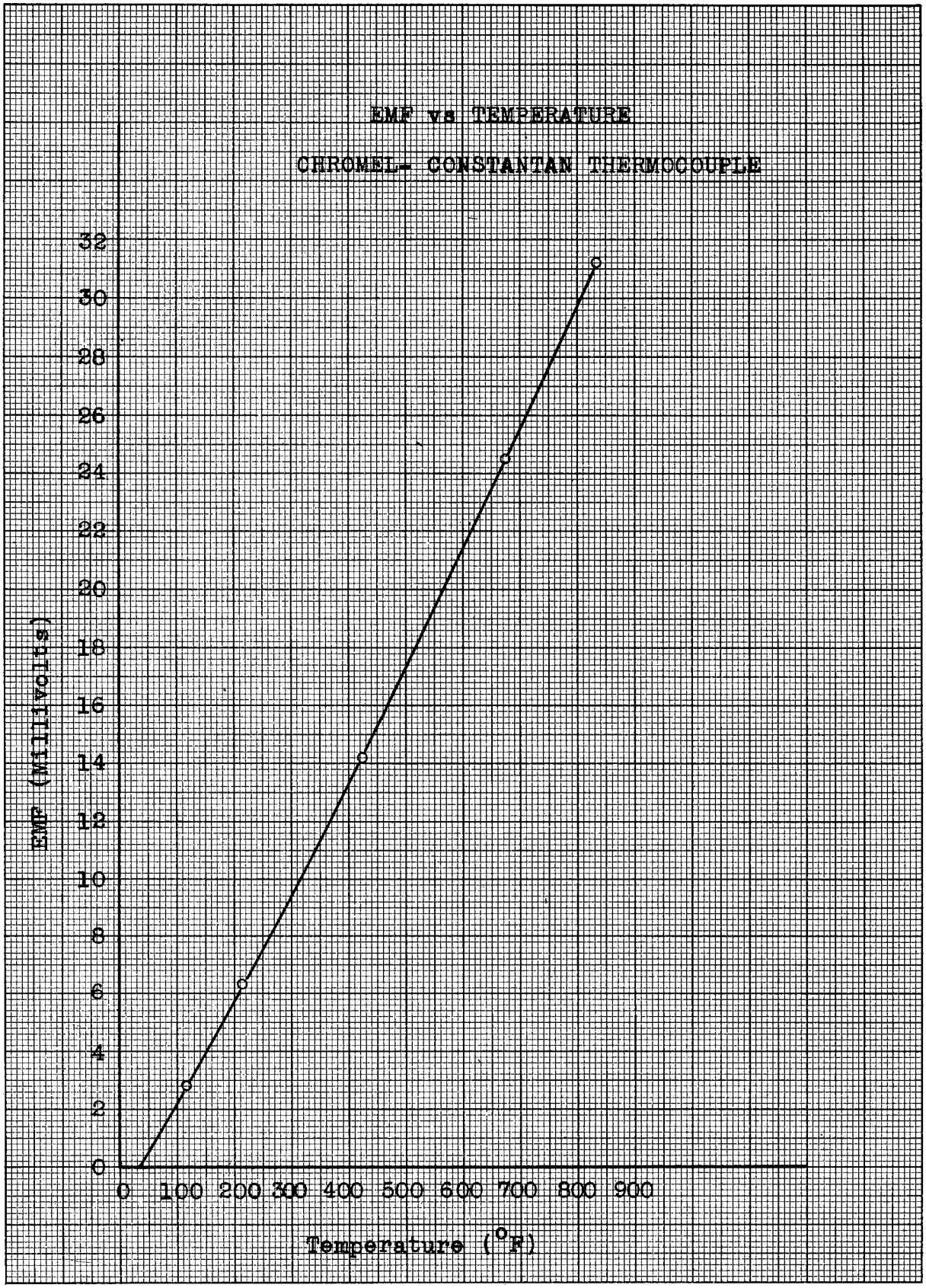

PVO
EHS
4/16/50

Fig. 25

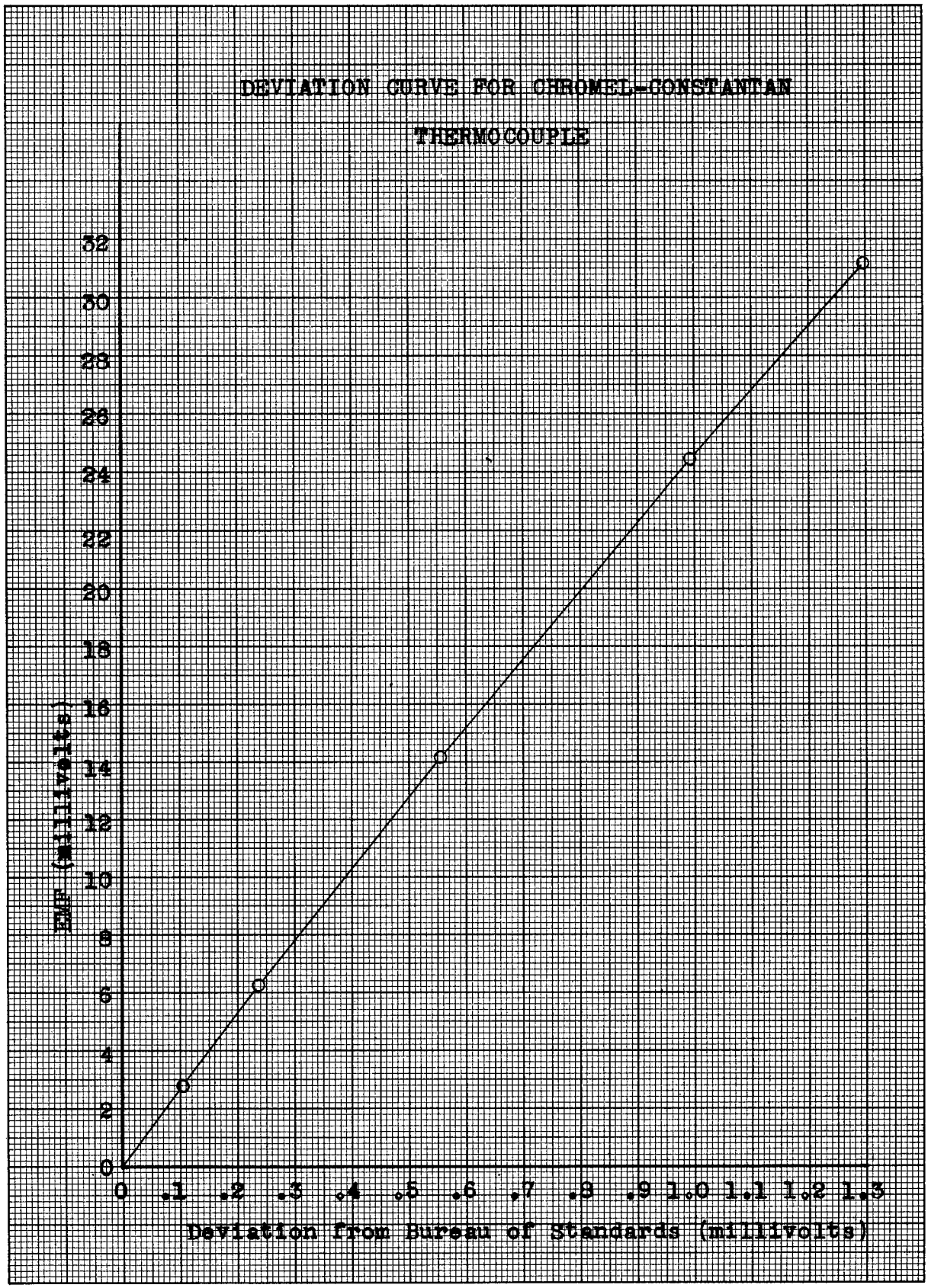

PVO
EHS
3/11/50

Fig. 26

TEST SECTION MOCK UP

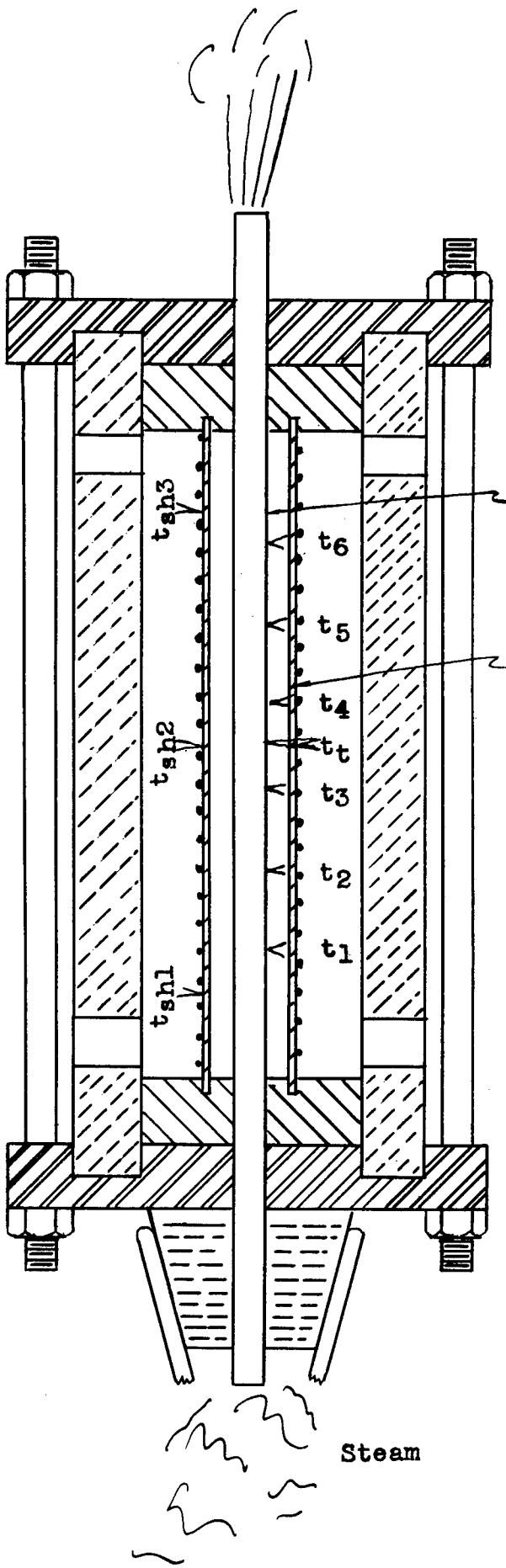

Nickel Tube
.180 in. I.D.
.210 in. O.D.

Heated Copper Shield

t_{1-6} Test Thermo.

t_{sh} Shield Thermo.

t_t Tube Thermo.

PVO
EHS
4/11/50

Fig. 27

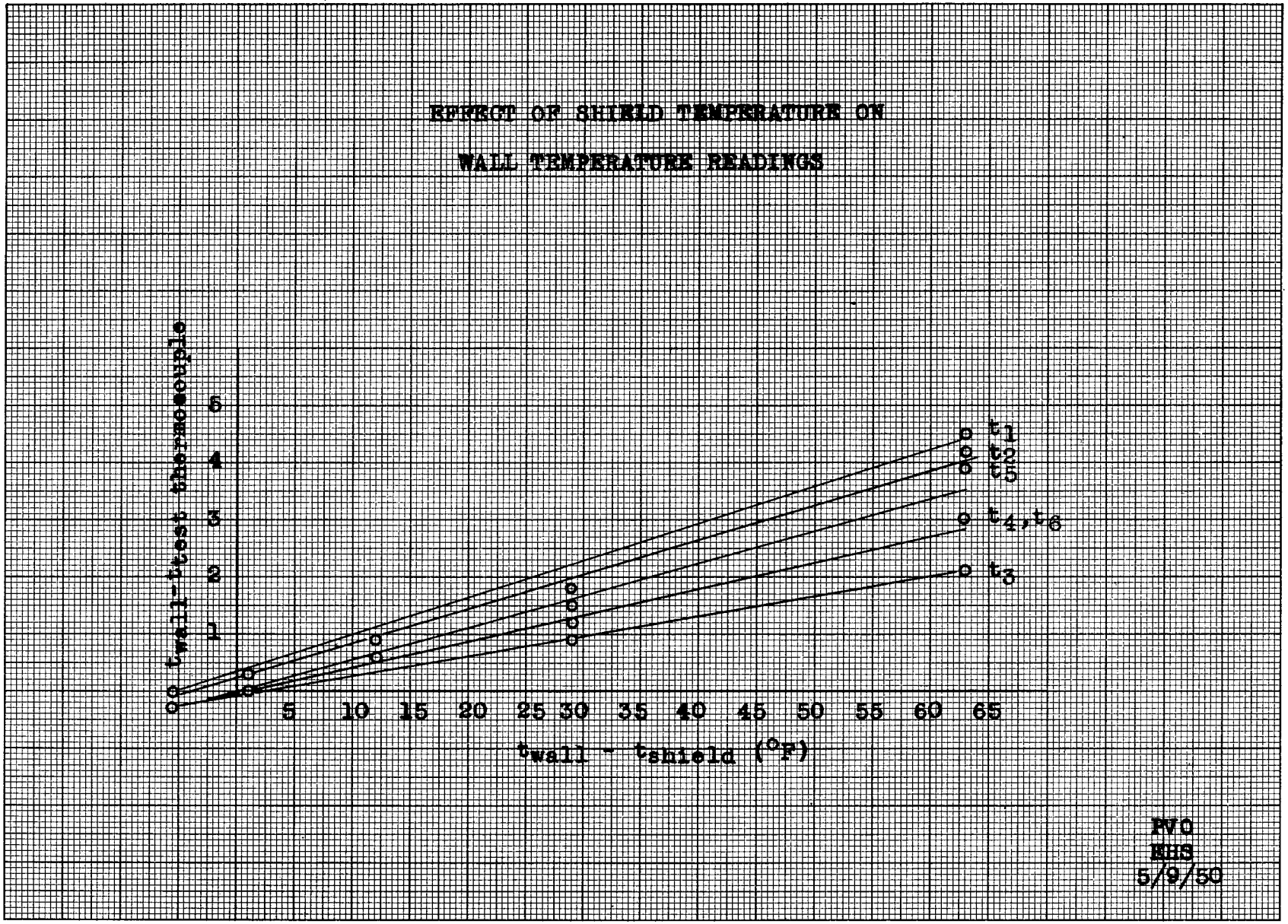
EFFECT OF SHIELD TEMPERATURE ON
WALL TEMPERATURE READINGS
t_{wall} - test thermocouple
1
2
3
4
5
5 10 15 20 25 30 35 40 45 50 55 60 65
$t_{wall} - t_{shield}$ (°F)
t_1
t_2
t_5
t_4, t_6
t_3
PVC
EHS
5/9/50

Fig. 28

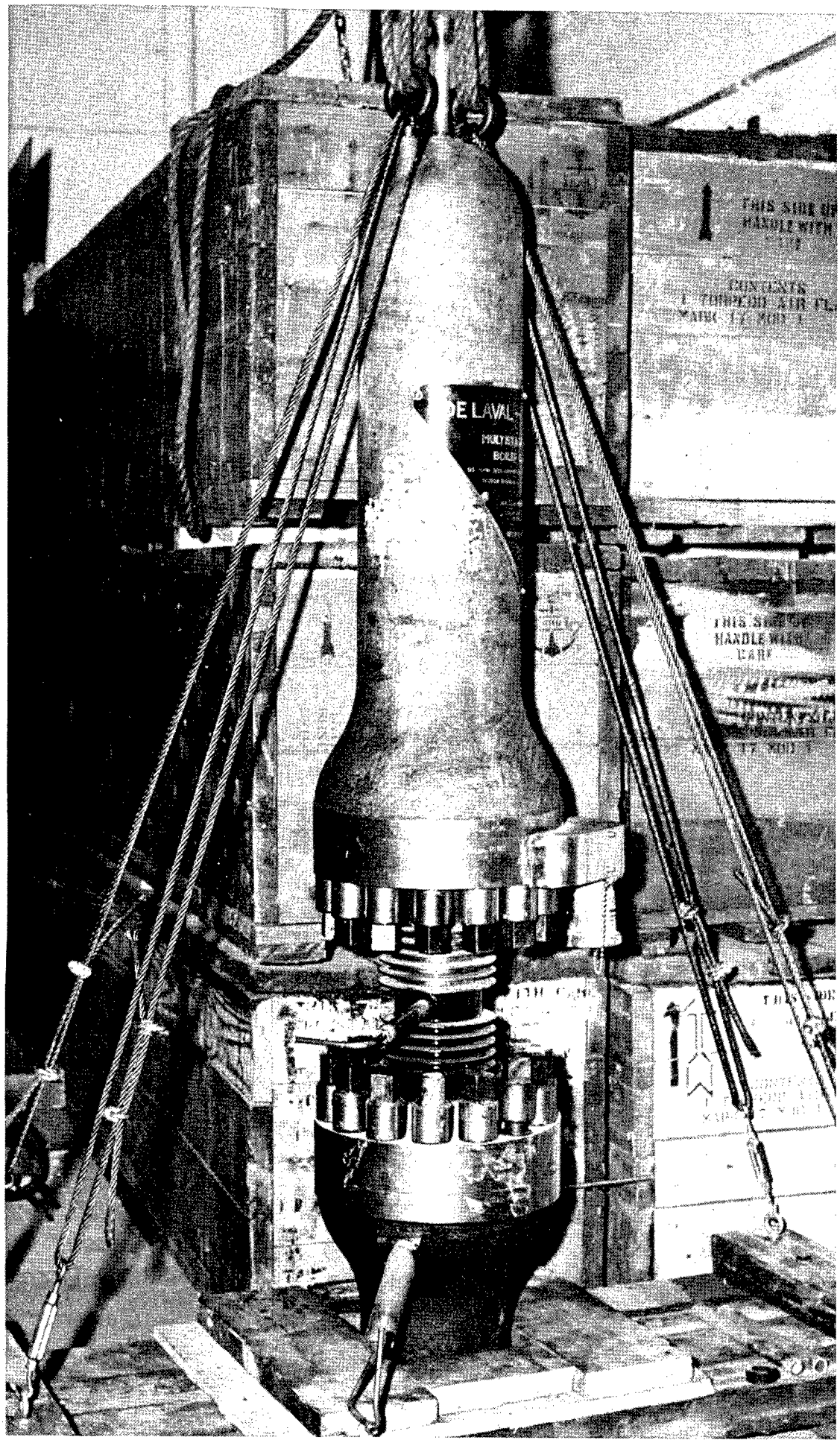

Fig. 29

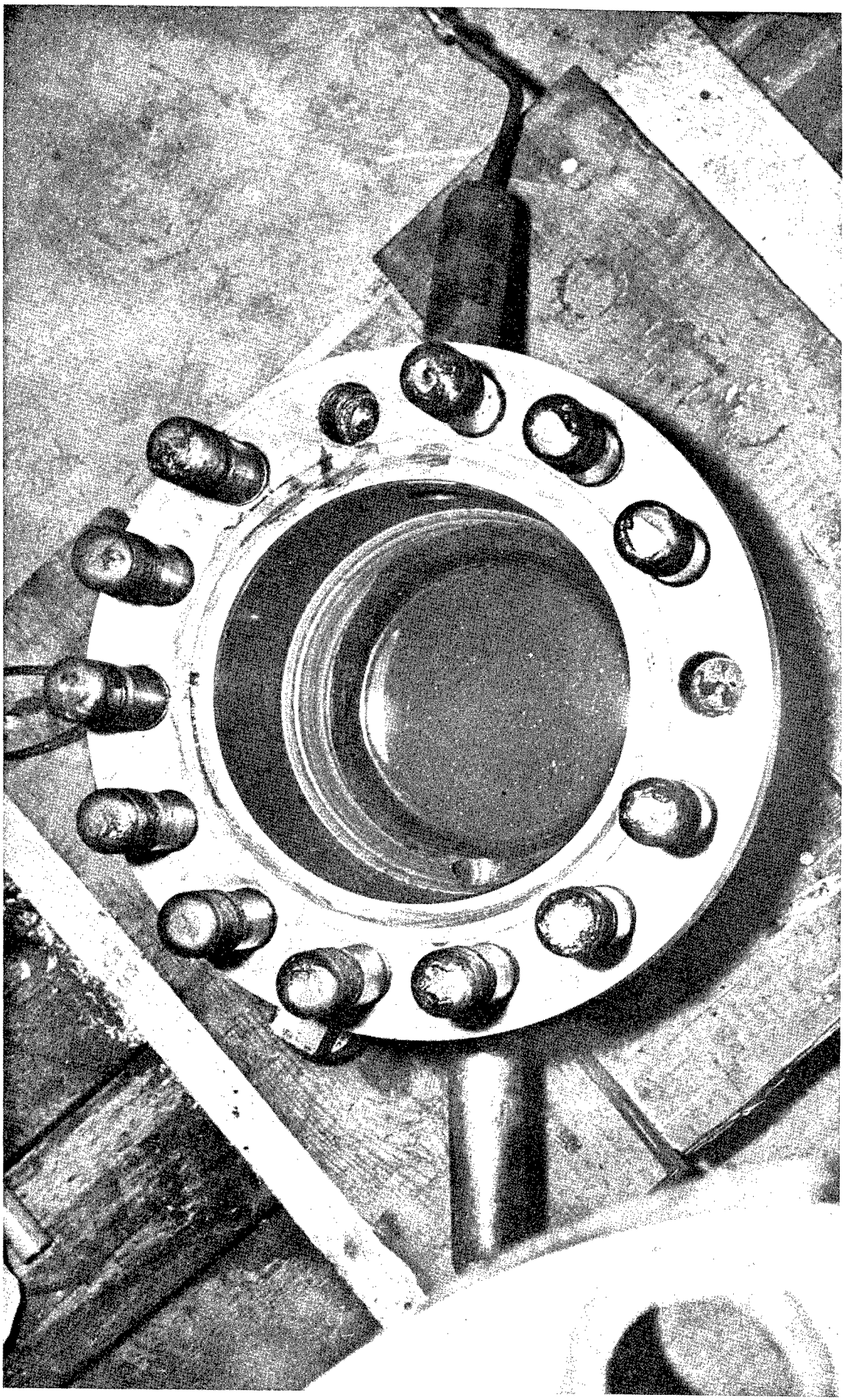

Fig. 30

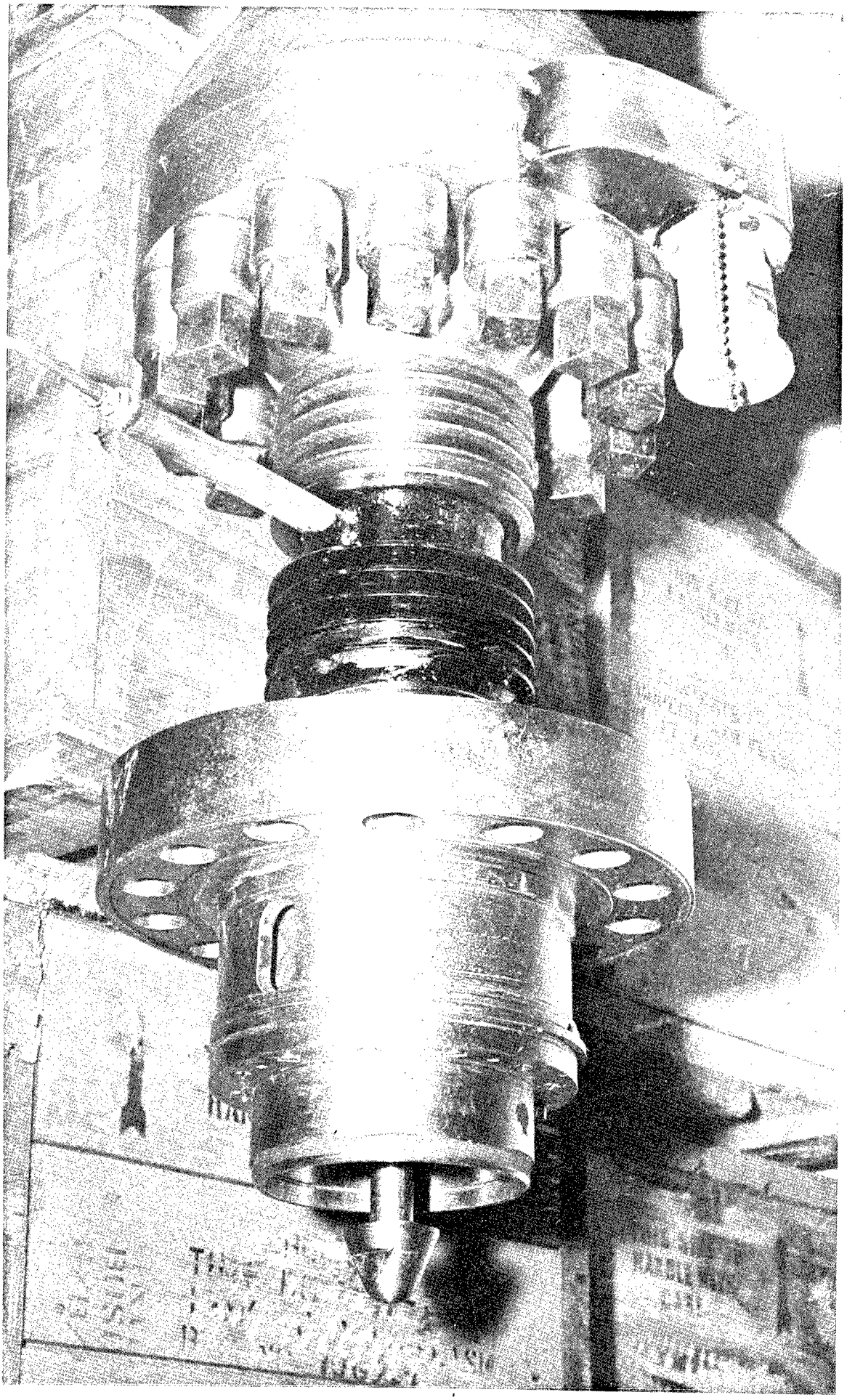

Fig. 31

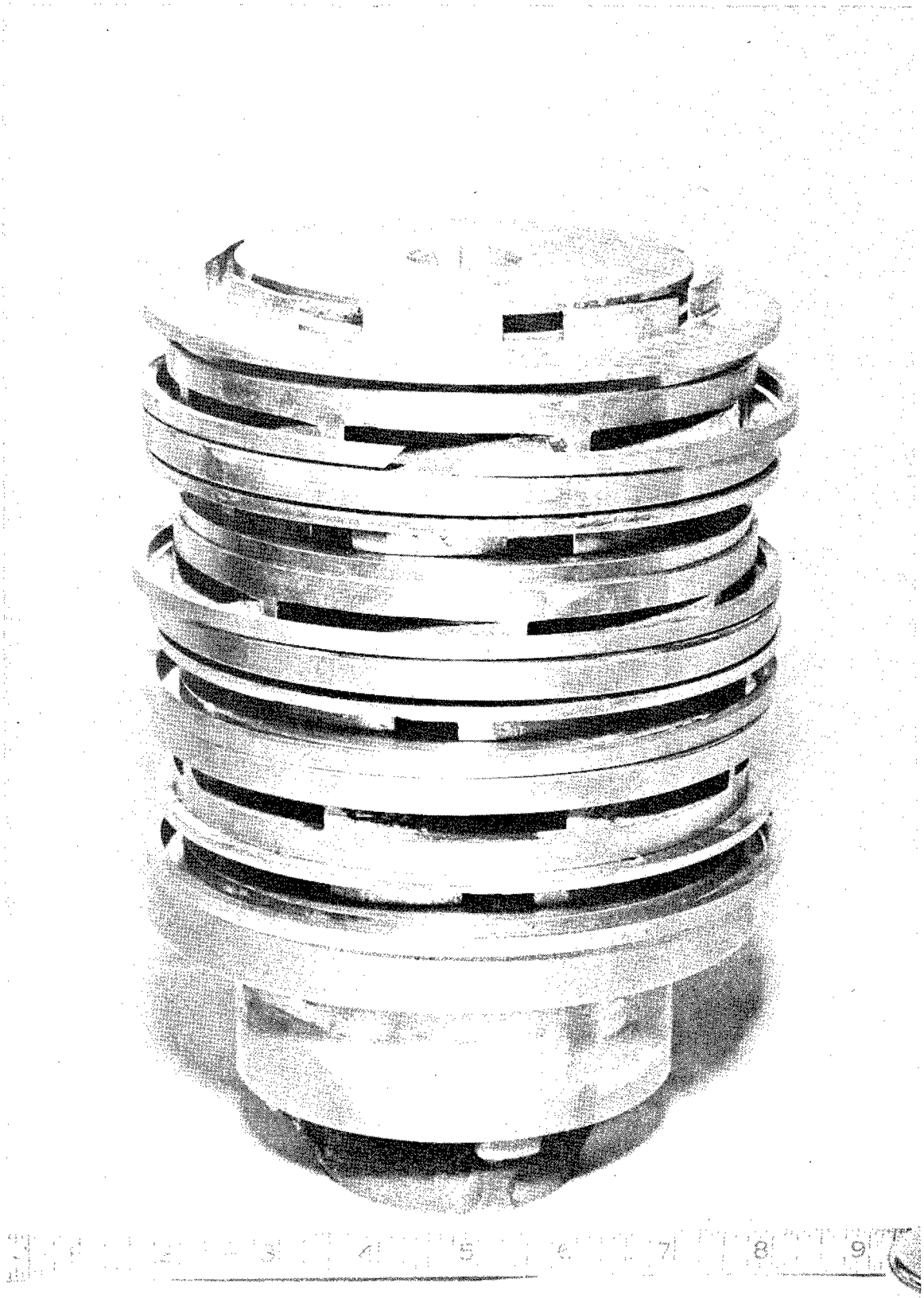

Fig. 32

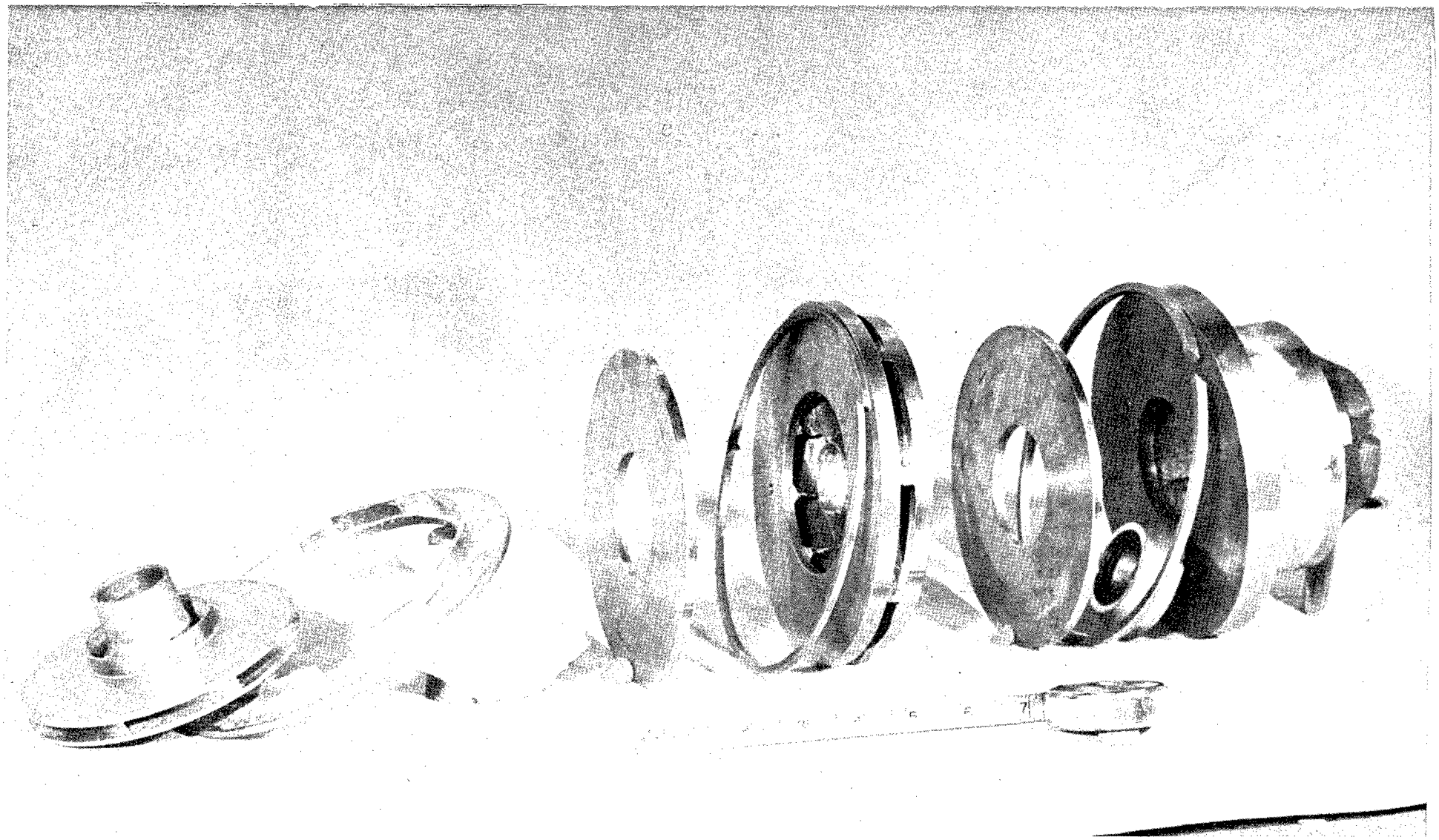

Fig. 33

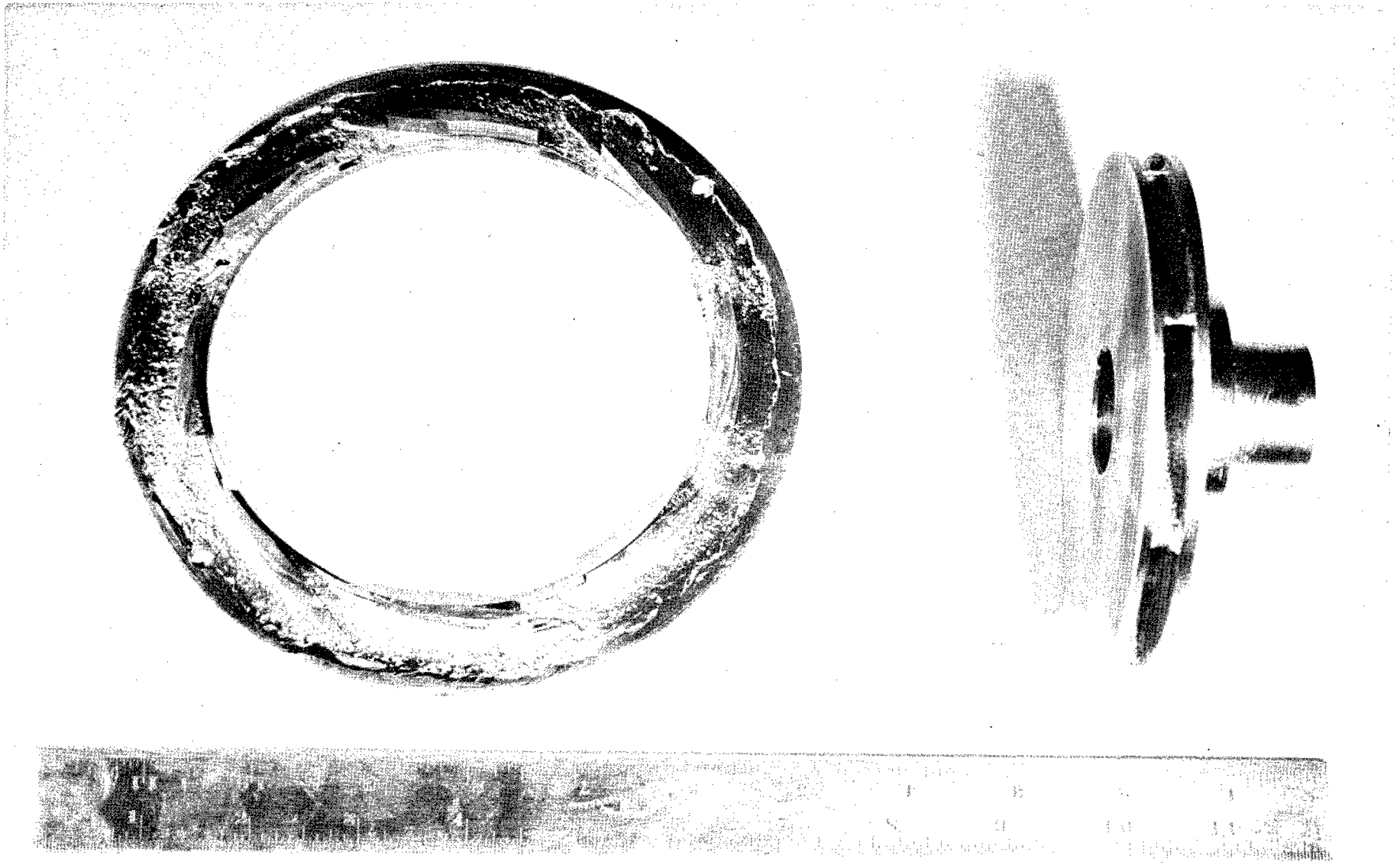

Fig. 34

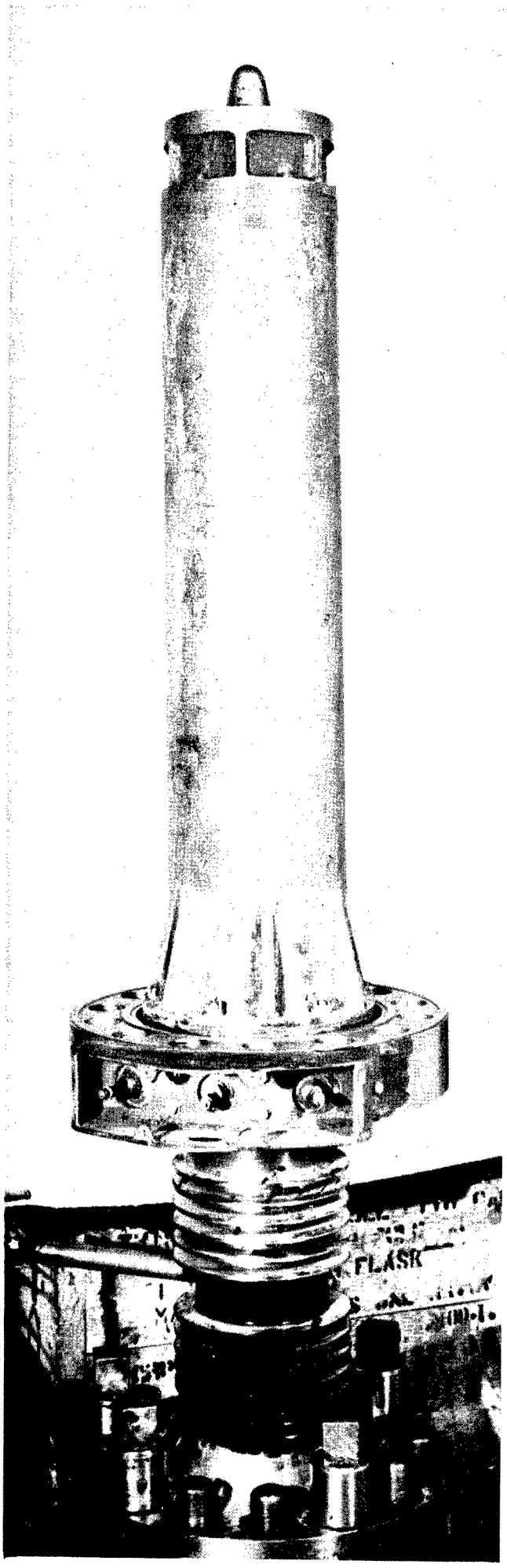

Fig. 35

Commanding Officer
Office of Naval Research
Branch Office
150 Causeway Street
Boston 14, Mass.

Commanding Officer
Office of Naval Research
Branch Office
346 Broadway
New York 13, N. Y.

Commanding Officer
Office of Naval Research
Branch Office
86[illegible] N. Rush Street
Chicago 11, Illinois

Commanding Officer
Office of Naval Research
Branch Office
1000 Geary Street
San Francisco 9[illegible], Calif.

Commanding Officer
Office of Naval Research
Branch Office
1030 Green Street
Pasadena, Calif. (3)

Contract Administrator, SE Area
Office of Naval Research
Department of the Navy
Washington 25, D. C.
Attn: Mr. L. F. Lynch (2)

Office of Chief of Ordnance
Research and Development Section
Department of the Army
The Pentagon
Washington 25, D. C.
Attn: ORDTB (1)

Commanding General
U. S. Air Force
The Pentagon
Washington 25, D. C.
Attn: Research & Development Div. (1)

Office of Air Research
Wright-Patterson Air Force Base
Dayton, Ohio
Attn: Chief, Applied Mechanics Group (1)

U. S. Atomic Energy Commission
Division of Research
Washington, D. C. (1)

Argonne National Laboratory
P. O. Box 5207
Chicago 80, Illinois
Attn: W. H. Jens (25)

U. S. Coast Guard
1300 E Street, N. W.
Washington, D. C.
Attn: Chief, Testing and Development
Division (1)

National Advisory Committee for
Aeronautics
Cleveland Municipal Airport
Cleveland, Ohio
Attn: J. H. Collins, Jr. (2)

Dr. William Sibbitt
Purdue Research Foundation
Purdue University
Lafayette, Indiana (1)

Professor E. D. Kane
University of California
Berkeley, California (1)

[illegible]
[illegible]
[illegible] (1)

Professor W. E. Edmonds
Department of Electrical Engineering
Massachusetts Institute of Technology
Cambridge 39, Massachusetts ( )

Professor A. T. Ippen
Department of Mechanical Engineering
Stanford University
Stanford, California ( )

Professor Warren Rohsenow
Mechanical Engineering Department
Massachusetts Institute of Technology
Cambridge 39, Massachusetts ( )

Mr. M. E. Turnbaugh
c/o U. S. Atomic Energy Commission
P. O. Box 1105
Pittsburgh 30, Pa. ( )

Mr. **C. Lynn**
Westinghouse Electric Co.
Atomic Power Division
P. O. Box 1468
Pittsburgh, Pa. ( )

Dean L. M. K. Boelter
Dept. of Engineering
University of California
Los Angeles, California ( )

Professor J. P. Keenan
Dept. of Mechanical Engr.
Mass. Inst. of Technology
Cambridge 39, Massachusetts ( )

Professor J. E. Addoms
Dept. of Chemical Engr.
Mass. Inst. of Technology
Cambridge 39, Mass. ( )

Dean W. J. Wohlenberg
School of Engineering
Yale University
New Haven, Conn. ( )

Mr. E. S. Kunn
Room 20-B-226
Mass. Inst. of Technology
Cambridge 39, Mass. ( )

S. Naymark

Mrs. V. Sternberg,

Distribution (cont.)

Officer in Charge
Office of Naval Research
Branch Office
Navy No. 100, Fleet P.O.
New York, N. Y. (5)